$\hbar$ corrections in semiclassical formulas for smooth chaotic dynamics

Benoît Grémaud*
Laboratoire Kastler Brossel, Université Pierre et Marie Curie, T12, E1 4, Place Jussieu 75252, Paris cedex 05, France
(Received 13 July 2001; published 30 April 2002)

The validity of semiclassical expansions in the power of $\hbar$ for the quantum Green's function have been extensively tested for billiards systems, but in the case of chaotic dynamics with smooth potential, even if formulas are existing, a quantitative comparison is still missing. In this paper, extending the theory developed by Gaspard *et al.* [Adv. Chem. Phys. **90**, 105 (1995)], based on the classical Green's functions, we present an efficient method allowing the calculation of $\hbar$ corrections for the propagator, the quantum Green's function, and their traces. In particular, we show that the previously published expressions for $\hbar$ corrections to the traces are incomplete.

DOI: 10.1103/PhysRevE.65.056207 PACS number(s): 05.45.Mt, 03.65.Sq

I. INTRODUCTION

Gutzwiller's work has now become a milestone in the understanding of the properties of a quantum system whose classical counterpart depicts chaotic dynamics [1]. Starting from Feynman's path formulation of quantum mechanics, he has been able to complete the early studies of Van Vleck [2], deriving expressions for the semiclassical propagator, and from this, for the quantum level density: the well-known Gutzwiller trace formula. The latter is an asymptotic series in $\hbar$ and can be separated into two parts; the leading order corresponds to the Thomas-Fermi (or extended Thomas-Fermi when including $\hbar$ corrections) average density of states [3]; the other part corresponds to the oscillations around the preceding term and involves contributions from all periodic orbits of the system. This formula has been widely used to obtain approximate values for the quantum energy eigenvalues of classically chaotic systems: the hydrogen atom in magnetic field [4,5], the helium atom [6–8], anisotropic Kepler problem [1], resonant tunnel diode [9], billiards [10–13], etc. Since then, the Gutzwiller trace formula has also been generalized to take into account contributions of other kinds: diffractive effects [14], continuous families of periodic orbits [13,15,16], ghost orbits, etc.

At the same time, because the trace formula as derived by Gutzwiller only contained the leading term of the asymptotic expansion of the quantum level density, the systematic expansion of the semiclassical propagator in powers of $\hbar$ has been the purpose of several studies [12,13,17]. However, these corrections to the trace formula have only been tested for billiards, for which both classical and quantum properties are easier to calculate. In the present paper, we will show how, for quantum systems whose Hamiltonian separates into kinetic and smooth potential energies, $\hbar$ corrections can be computed with great accuracy, extending the method described in Refs. [12,13], based on classical Green's functions. In particular, we will show that the previous derivation [12,13] of the correction to Gutzwiller trace formula is partially wrong.

From a numerical point of view, all quantities involved in the calculation of the $\hbar$ corrections for a given classical path can be obtained as solutions of sets of first order differential equations to be integrated along this path using standard time integrators like the Runge-Kutta method. The number of equations in these sets can be quite large and can be probably reduced with a deeper analysis of their structures, in the same way that the amplitude in the Gutzwiller trace formula for a two-dimensional (2D) system can be obtained by integrating only a (2×2) matrix and not the whole monodromy matrix [18]. However, it would give rise to more complicated expressions and probably to additional difficulties in the numerical implementation, whereas the expressions given in the paper can be put in the computer as they stand. Also, the amount of CPU time and the memory needed by the codes are small enough, so that, on a first stage, the reduction of the number of equations can be skipped.

The paper is divided as follows. In Sec. II, expressions for the classical Green's functions involved in the $\hbar$ correction to the semiclassical propagator $K(\mathbf{q},\mathbf{q}_0,T)$ are derived. Then, we explain how to get a numerical implementation of these formulas allowing an efficient computation of the $\hbar$ correction. In Sec. III, we develop a numerical method to get the additional terms, arising from the time to energy domain transformation, in $\hbar$ correction for the quantum Green's function $G(\mathbf{q},\mathbf{q}_0,T)$. In the case of the trace of the propagator, essential steps for the derivation of the $\hbar$ correction are described in Sec. IV, leading to the proper formulas, along with the way they can be computed. The time to energy transformation is explained in Sec. V, leading to the $\hbar$ correction expression in the case of the quantum Green's function. Finally, Sec. VI shows how to apply theoretical expressions obtained in the four preceding sections in the case of the 2D hydrogen in magnetic field and emphasizes the excellent agreement with numerical coefficients extracted from exact quantum calculation, using harmonic inversion [19–21].

II. THE PROPAGATOR $K(\mathbf{q},\mathbf{q}_0,T)$

A. Feynman path integral

The starting point is the Feynman path integral, whose discrete version, for a time independent Hamiltonian which

*Electronic address: Benoit.Gremaud@spectro.jussieu.fr

separates into kinetic and potential energies, $\hat{H}=\hat{\mathbf{p}}^2/2+V(\hat{\mathbf{q}})$, reads as follows [13]:

$$K(\mathbf{q},\mathbf{q}_0,T)=\int d\mathbf{q}_1 d\mathbf{q}_2,\ldots,d\mathbf{q}_{N-1}(2\pi i\hbar\Delta t)^{-Nf/2}\times\exp\left[\frac{i}{\hbar}\sum_{n=0}^{N-1}L\left(\frac{\mathbf{q}_{n+1}-\mathbf{q}_n}{\Delta t},\mathbf{q}_n\right)\Delta t+O(\Delta t)\right], \tag{1}$$

where $\Delta t=T/N$, $\mathbf{q}_N=\mathbf{q}$, and $L(\dot{\mathbf{q}},\mathbf{q})$ is the classical Lagrangian.

For small values of $\hbar$ (i.e., the semiclassical limit), using the stationary phase approximation, all preceding integrals are expanded around the stationary solutions, that is the classical orbits $\mathbf{q}_l^{\mathrm{cl}}(t)$ going from $\mathbf{q}_0$ to $\mathbf{q}$ during time T, each of them thus giving a contribution $K_l(\mathbf{q},\mathbf{q}_0,T)$ to the propagator, whose final expression reads formally as follows [13]:

$$K_l(\mathbf{q},\mathbf{q}_0,T)=K_l^{(0)}(\mathbf{q},\mathbf{q}_0,T)\{1+i\hbar C_1(\mathbf{q},\mathbf{q}_0,T)+O(\hbar^2)\}, \tag{2}$$

where $K_l^{(0)}(\mathbf{q},\mathbf{q}_0,T)$ is the dominant semiclassical contribution to the propagator $K(\mathbf{q},\mathbf{q}_0,T)$:

$$K_l^{(0)}(\mathbf{q},\mathbf{q}_0,T)=\frac{1}{(2\pi i\hbar)^{f/2}}\left|\det\left(-\frac{\partial^2}{\partial\mathbf{q}\partial\mathbf{q}_0}W_l^{\mathrm{cl}}(\mathbf{q},\mathbf{q}_0,T)\right)\right|^{1/2}\times\exp\left[\frac{i}{\hbar}W_l^{\mathrm{cl}}(\mathbf{q},\mathbf{q}_0,T)-i\frac{\pi}{2}\nu_l\right], \tag{3}$$

where $W_l^{\mathrm{cl}}(\mathbf{q},\mathbf{q}_0,T)$ is the classical action and ν_l is the Morse index of the orbit. The $C_1(\mathbf{q},\mathbf{q}_0,T)$ expression is given by [13]

$$\frac{1}{8}\int_0^T dt\,V_{ijkl}^{(4)}(t)\mathcal{G}_{ij}(t,t)\mathcal{G}_{kl}(t,t)+\frac{1}{24}\int_0^T\int_0^T dt\,dt'\,V_{ijk}^{(3)}(t)V_{lmn}^{(3)}(t')\times[3\mathcal{G}_{ij}(t,t)\mathcal{G}_{kl}(t,t')\mathcal{G}_{mn}(t',t')+2\mathcal{G}_{il}(t,t')\mathcal{G}_{jm}(t,t')\mathcal{G}_{kn}(t,t')], \tag{4}$$

where the $V^{(n)}(t)$ are higher-order derivatives of the potential V, evaluated at $\mathbf{q}_l^{\mathrm{cl}}(t)$.

The classical Green's function $\mathcal{G}(t,t')$, associated with the classical orbit, is an $(f\times f)$ matrix solution of the following equation [13]:

$$\mathcal{D}\cdot\mathcal{G}(t,t')=\mathbb{1}\delta(t-t'), \tag{5}$$

where $\mathcal{D}$ is the Jacobi-Hill operator, controlling the linear stability around the classical orbit in the configuration space [13]

$$\mathcal{D}=-\frac{\mathrm{d}^2}{\mathrm{d}t^2}\mathbb{1}-\frac{\partial^2 V}{\partial\mathbf{q}\partial\mathbf{q}}[\mathbf{q}^{\mathrm{cl}}(t)]. \tag{6}$$

Furthermore, the fact that both initial and final point are fixed in the propagator $K(\mathbf{q},\mathbf{q}_0,T)$ imposes the following boundary conditions on the classical Green's function [13]:

$$\mathcal{G}(0,t')=\mathcal{G}(T,t')=0 \quad \forall\, t'\in[0,T]. \tag{7}$$

B. Classical Green's function

If $\mathbf{q}_l(T)$ is a conjugate point of $\mathbf{q}_0$, then the determinant $\det(-\partial^2_{\mathbf{q}\mathbf{q}_0}W_l^{\mathrm{cl}})$ in formula (3) is formally infinite, but this happens only for restricted values of T, so that, in this section, we will focus on the general case, for which $\mathbf{q}_l(T)$ and $\mathbf{q}_0$ are not conjugate points.

Apart from $t=t'$, $\mathcal{G}(t,t')$ obeying the homogeneous Jacobi-Hill equation $\mathcal{D}\cdot\mathcal{G}=0$, so that, introducing the notations

$$\mathcal{G}_-(t,t')=\mathcal{G}(t,t') \quad \text{for } 0\leqslant t\leqslant t',$$
$$\mathcal{G}_+(t,t')=\mathcal{G}(t,t') \quad \text{for } t'\leqslant t\leqslant T, \tag{8}$$

one immediately obtains

$$\begin{pmatrix}\mathcal{G}_\pm(t,t')\\ \dot{\mathcal{G}}_\pm(t,t')\end{pmatrix}=M(t)\begin{pmatrix}A_\pm(t')\\ B_\pm(t')\end{pmatrix}, \tag{9}$$

where $M(t)$ is the $(2f\times 2f)$ monodromy matrix, depicting the linear stability around the classical orbit in the phase space. $A_\pm$ and $B_\pm$ are four $(f\times f)$ matrices, whose values are determined from the boundary conditions at time $t=t'$:

$$\mathcal{G}_+(t',t')-\mathcal{G}_-(t',t')=0,$$
$$\frac{d\mathcal{G}_-}{dt}(t',t')-\frac{d\mathcal{G}_+}{dt}(t',t')=\mathbb{1} \tag{10}$$

and at times $t=0$ and $t=T$:

$$\mathcal{G}_-(0,t')=0,$$
$$\mathcal{G}_+(T,t')=0. \tag{11}$$

For a Hamiltonian which separates between kinetic and potential energy $H=\mathbf{p}^2/2+V(\mathbf{q})$, $M(t)$ has the following simple structure:

$$M(t)=\begin{bmatrix}J_2(t) & J_1(t)\\ \dot{J}_2(t) & \dot{J}_1(t)\end{bmatrix}, \tag{12}$$

which leads us to the following explicit expressions for the four matrices $A_\pm$ and $B_\pm$:

$$
\begin{aligned}
&A_-(t')=0,\\
&B_-(t')=J_2^\top(t')-J_1^{-1}(T)J_2(T)J_1^\top(t'),\\
&A_+(t')=J_1^\top(t'),\\
&B_+(t')=-J_1^{-1}(T)J_2(T)J_1^\top(t'),
\end{aligned}
\tag{13}
$$

provided that $J_1^{-1}(T)$ is invertible. $J_1(T)$ being the upper right $(f\times f)$ submatrix of the matrix M, gives the linear displacement of the final position for a change in the initial momentum (the initial position being fixed to $\mathbf{q}_0$), i.e., $\delta\mathbf{q}(T)=J_1(T)\,\delta\mathbf{p}_0$. Thus, $J_1(T)$ is the inverse matrix of $(-\partial^2_{\mathbf{q}\mathbf{q}_0}W_l^{\mathrm{cl}})$ which has been supposed to be invertible [$\mathbf{q}(T)$ and $\mathbf{q}_0$ are not conjugate points]. Finally, the full expression for the classical Green's function reads

$$
\mathcal{G}(t,t')=\begin{cases} J_1(t) & [J_2^\top(t')-J_1^{-1}(T)J_2(T)J_1^\top(t')] \quad \text{for } 0\leqslant t\leqslant t',\\ [J_2(t)-J_1(t)J_1^{-1}(T)J_2(T)] & J_1^\top(t') \quad \text{for } t'\leqslant t\leqslant T. \end{cases}
\tag{14}
$$

Using the symplectic structure of $M(T)$, one can show that

$$
\mathcal{G}(t',t)=\mathcal{G}^\top(t,t')
\tag{15}
$$

as expected because the operator $\mathcal{D}$ and the boundary conditions are symmetric as it explicitly appears in the discrete version of the problem (see Ref. [13]). This is also emphasized in Fig. 1, where the four matrix elements of a classical Green's function $\mathcal{G}(t,t')$ (for $t'/T=0.6$) are plotted with respect to time t. This example corresponds to a classical orbit of the 2D hydrogen atom in a magnetic field having initial and final points on the nucleus, namely, the closed orbit having code 0—and whose trajectory in (u,v) coordinates is also shown in the figure. (See Sec. VI for all details.) As expected, the Green's function vanishes at initial and final times [i.e., $\mathcal{G}(0,t')=\mathcal{G}(T,t')=0$] and for $t=t'$, the derivatives of each diagonal element $\mathcal{G}_{11}(t',t')$ (continuous line) and $\mathcal{G}_{22}(t',t')$ (long dashed line) are discontinuous whereas, from property (15), the two off-diagonal elements are equal (dotted and dashed lines).

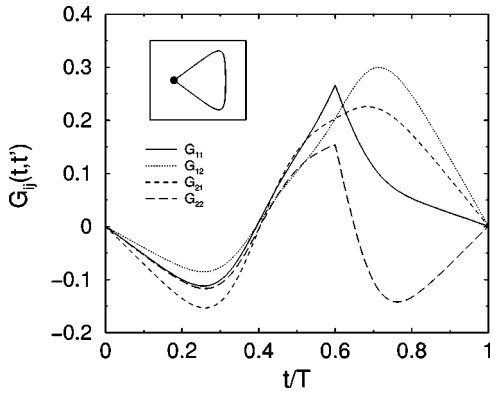

FIG. 1. Example of a classical Green's function $\mathcal{G}(t,t')$ involved in the calculation of the $\hbar$ corrections for the propagator $K(\mathbf{q},\mathbf{q}_0,T)$, for the case $\mathbf{q}=\mathbf{q}_0=\mathbf{0}$. It is associated with the closed orbit 1243 of the 2D hydrogen atom in magnetic field, whose trajectory in (u,v) coordinates is inserted in the plot (see Sec. VI for all details). This trajectory starts and ends at the nucleus, depicted by the black circle. Each curve corresponds to a matrix element $\mathcal{G}_{ij}(t,t')$ plotted with respect to time t, for $t'/T=0.6$. As expected from boundary conditions (7), the Green's function vanishes at initial and final times [i.e., $\mathcal{G}(0,t')=\mathcal{G}(T,t')=0$] and for $t=t'$, the derivatives of diagonal elements, $\mathcal{G}_{11}(t',t')$ (continuous line) and $\mathcal{G}_{22}(t',t')$ (long dashed line), are discontinuous whereas, from symmetry property (15) [i.e., $\mathcal{G}^\top(t,t')=\mathcal{G}(t',t)$], the two off-diagonal elements are equal (dotted and dashed lines).

C. Getting $C_1(\mathbf{q},\mathbf{q}_0,T)$ by integrating a set of first order differential equations

From Eq. (4), there are three contributions to $C_1(\mathbf{q},\mathbf{q}_0,T)$, namely,

$$
\begin{aligned}
I_1(T)&=\int_0^T dt\, V^{(4)}_{ijkl}(t)\mathcal{G}_{ij}(t,t)\mathcal{G}_{kl}(t,t),\\
I_2^+(T)&=\int_0^T\int_0^T dt\,dt'\,V^{(3)}_{ijk}(t)V^{(3)}_{lmn}(t')\\
&\quad\times\mathcal{G}_{ij}(t,t)\mathcal{G}_{kl}(t,t')\mathcal{G}_{mn}(t',t'),\\
I_2^-(T)&=\int_0^T\int_0^T dt\,dt'\,V^{(3)}_{ijk}(t)V^{(3)}_{lmn}(t')\\
&\quad\times\mathcal{G}_{il}(t,t')\mathcal{G}_{jm}(t,t')\mathcal{G}_{kn}(t,t').
\end{aligned}
\tag{16}
$$

Even if, in principle, one can compute $\mathcal{G}(t,t')$ for any (t,t') values using Eq. (14), direct evaluation of the double integrals $I_2^\pm$ would be time consuming and numerically inefficient using standard integration routines, especially because, from its definition, $\mathcal{G}(t,t')$ is not a smooth function around the line $t=t'$. In what follows, we will show that the preceding integrals can be transformed in such a way that their values can be obtained integrating a set of first order differential equations along the classical orbit, in the same way that, for example, the monodromy matrix $M(T)$ can be computed.

Separating $t>t'$ and $t<t'$ contributions in $I_2^{\pm}$, using symmetry property (15) of $\mathcal{G}(t,t')$ and that the matrix $V^{(3)}$ is fully symmetric under index permutations, one gets, after straightforward algebra,

$$I_2^+(T)=2\int_0^T dt\int_0^t dt'\; V^{(3)}_{ijk}(t)V^{(3)}_{lmn}(t')\times\mathcal{G}_{ij}(t,t)\mathcal{G}_{kl}(t,t')\mathcal{G}_{mn}(t',t'),$$

$$I_2^-(T)=2\int_0^T dt\int_0^t dt'\; V^{(3)}_{ijk}(t)V^{(3)}_{lmn}(t')\times\mathcal{G}_{il}(t,t')\mathcal{G}_{jm}(t,t')\mathcal{G}_{kn}(t,t'). \quad (17)$$

In the preceding expressions the Green's function $\mathcal{G}(t,t')$ is used only for (t,t') values in the triangle $0\leqslant t'\leqslant t\leqslant T$ and is formally written $\mathcal{G}(t,t')=B_-^{\top}(t)J_1^{\top}(t')$ [see Eq. (14)], thus separating t and t' contributions:

$$I_2^+(T)=2\int_0^T dt\; V^{(3)}_{ijk}(t)\mathcal{G}_{ij}(t,t)B^-_{pk}(t)\times\int_0^t dt'\; V^{(3)}_{lmn}(t')J_{1lp}(t')\mathcal{G}_{mn}(t',t'),$$

$$I_2^-(T)=2\int_0^T dt\; V^{(3)}_{ijk}(t)B^-_{pi}(t)B^-_{qj}(t)B^-_{rk}(t)\times\int_0^t dt'\; V^{(3)}_{lmn}(t')J_{1lp}(t')J_{1mq}(t')J_{1nr}(t'). \quad (18)$$

This leads us to introduce two intermediate quantities, namely, $P_p(t)$ and $Q_{pqr}(t)$ (for p, q and r running from 1 to f):

$$P_p(t)=\int_0^t dt'\; V^{(3)}_{lmn}(t')J_{1lp}(t')\mathcal{G}_{mn}(t',t'),$$

$$Q_{pqr}(t)=\int_0^t dt'\; V^{(3)}_{lmn}(t')J_{1lp}(t')J_{1mq}(t')J_{1nr}(t') \quad (19)$$

in a way such that $I_2^{\pm}(T)$ [and $I_1(T)$] are solutions of the following set of differential equations [besides equations for $\mathbf{X}(t)$ and $M(t)$]:

$$\begin{aligned}
\dot I_1&=V^{(4)}_{ijkl}(t)\mathcal{G}_{ij}(t,t)\mathcal{G}_{kl}(t,t),\\
\dot P_p&=V^{(3)}_{lmn}(t)J_{1lp}(t)\mathcal{G}_{mn}(t,t),\\
\dot I_2^+&=V^{(3)}_{ijk}(t)\mathcal{G}_{ij}(t,t)B^-_{pk}(t)P_p(t),\\
\dot Q_{pqr}&=V^{(3)}_{lmn}(t)J_{1lp}(t)J_{1mq}(t)J_{1nr}(t),\\
\dot I_2^-&=V^{(3)}_{ijk}(t)B^-_{pi}(t)B^-_{qj}(t)B^-_{rk}(t)Q_{pqr}(t)
\end{aligned} \quad (20)$$

with initial conditions $I_1(0)=I_2^{\pm}(0)=P_p(0)=Q_{pqr}(0)=0$. This set of equations, f^3+4f^2+3f+3 in total (i.e., 33 for a 2D system) is easily integrated using any standard method (fourth order Runge-Kutta in the present case). As mentioned in the Introduction, the size of the preceding differential set is probably not minimal and could be reduced by a deeper analysis of the structure of these equations. However, it allows a fast and easy computation of the correction $C_1(\mathbf{q},\mathbf{q}_0,T)$:

(1) find a trajectory going from $\mathbf{q}_0$ to $\mathbf{q}$ in time T;

(2) integrate the differential set for $\mathbf{X}(t)$ and $M(t)$ along the trajectory to obtain the quantity $J_1^{-1}(T)J_2(T)$;

(3) integrate the set of Eqs. (20) along the trajectory to get the three quantities I_1, $I_2^{\pm}$, entering in the $C_1(\mathbf{q},\mathbf{q}_0,T)$ expression.

III. THE GREEN'S FUNCTION $G(\mathbf{q},\mathbf{q}_0,E)$

A. Going from time to energy domain

Since the quantum Green's function $G(\mathbf{q},\mathbf{q}_0,E)$ is related to the propagator $K(\mathbf{q},\mathbf{q}_0,T)$, through a semisided Fourier transform, this relation also holds between semiclassical contributions arising from each classical orbit, more precisely,

$$G_l(\mathbf{q},\mathbf{q}_0,E)=\frac{1}{i\hbar}\int_0^{+\infty}dT\exp\left(\frac{i}{\hbar}ET\right)K_l(\mathbf{q},\mathbf{q}_0,T). \quad (21)$$

Again, a stationary phase approximation is used to perform the integral, which, for a given trajectory going from $\mathbf{q}_0$ to $\mathbf{q}$, selects its total duration T_0 such that the classical motion is made at energy E. This operation also gives rise to additional terms in $\hbar$ corrections, to be summed with $C_1(\mathbf{q},\mathbf{q}_0,T)$, and whose explicit expressions can be derived starting from Eq. (4) formally written as follows [13]:

$$K_l(\mathbf{q},\mathbf{q}_0,T)=\frac{1}{(2\pi i\hbar)^{f/2}}\exp\left[\frac{i}{\hbar}W_l(\mathbf{q},\mathbf{q}_0,T)-i\frac{\pi}{2}\nu_l+C_0(\mathbf{q},\mathbf{q}_0,T)+i\hbar C_1(\mathbf{q},\mathbf{q}_0,T)\right], \quad (22)$$

$C_0(\mathbf{q},\mathbf{q}_0,T)$ being the (logarithm of) usual semiclassical amplitude. Then $W_l(\mathbf{q},\mathbf{q}_0,T)$ and $C_0(\mathbf{q},\mathbf{q}_0,T)$ are systematically expanded around T_0:

$$\begin{aligned}
W_l(\mathbf{q},\mathbf{q}_0,T)&=W_l^{(0)}+\delta T\,W_l^{(1)}+\frac{\delta T^2}{2}W_l^{(2)}+\frac{\delta T^3}{6}W_l^{(3)}+\frac{\delta T^4}{24}W_l^{(4)},\\
C_0(\mathbf{q},\mathbf{q}_0,T)&=C_0^{(0)}+\delta T\,C_0^{(1)}+\frac{\delta T^2}{2}C_0^{(2)},
\end{aligned} \quad (23)$$

with $\delta T=(T-T_0)$. Terms arising from $C_1(T)$ expansion would contribute only to $\hbar^2$ correction and can be discarded. Performing the imaginary Gaussian integrals leads to the additional $\hbar$ corrections:

$$C_1^{T\to E}(\mathbf{q},\mathbf{q}_0,T_0)=\frac{1}{2W_l^{(2)}}[(C_0^{(1)})^2+C_0^{(2)}] -\frac{W_l^{(3)}C_0^{(1)}}{2(W_l^{(2)})^2}-\frac{W_l^{(4)}}{8(W_l^{(2)})^2}+\frac{5}{24}\frac{(W_l^{(3)})^2}{(W_l^{(2)})^3}. \tag{24}$$

The preceding formula is similar to the one in Ref. [13], where the authors have expressed the coefficient $C_1^{T\to E}(\mathbf{q},\mathbf{q}_0,T_0)$ in terms of derivatives of amplitude and action with respect to energy E. The full expression of $G_l(\mathbf{q},\mathbf{q}_0,E)$ is then given by

$$G_l(\mathbf{q},\mathbf{q}_0,E)=\frac{2\pi}{(2\pi i\hbar)^{(f+1)/2}}\frac{1}{|W_l^{(2)}\det J_1(T_0)|^{1/2}} \times\exp\left[\frac{i}{\hbar}S_l(\mathbf{q},\mathbf{q}_0,E)-i\frac{\pi}{2}\tilde{\nu}_l\right] \times\{1+i\hbar[C_1(\mathbf{q},\mathbf{q}_0,T_0)+C_1^{T\to E}(\mathbf{q},\mathbf{q}_0,T_0)] +O(\hbar^2)\}, \tag{25}$$

where $S_l(\mathbf{q},\mathbf{q}_0,E)$ is the reduced action and

$$\tilde{\nu}_l=\nu_l \quad \text{if } W_l^{(2)}>0, \qquad \tilde{\nu}_l=\nu_l+1 \quad \text{if } W_l^{(2)}<0. \tag{26}$$

B. Getting $C_1^{T\to E}(\mathbf{q},\mathbf{q}_0,T_0)$ by integrating a set of first order differential equations

In Sec. II C, we have shown that $C_1(\mathbf{q},\mathbf{q}_0,T_0)$ can be computed by integrating a set of differential equations along the classical orbit going from $\mathbf{q}_0$ to $\mathbf{q}$ in time T_0. In this section we will show that it is also true for $C_1^{T\to E}(\mathbf{q},\mathbf{q}_0,T_0)$, which involves derivatives of both $W_l(\mathbf{q},\mathbf{q}_0,T)$ and $\det J_1(T)$ with respect to T.

For all T, we have the following functional relation ($\mathbf{q}_0$ and $\mathbf{q}$ being fixed):

$$\frac{\partial W_l(\mathbf{q},\mathbf{q}_0,T)}{\partial T}=-E(\mathbf{q},\mathbf{q}_0,T), \tag{27}$$

where $E(\mathbf{q},\mathbf{q}_0,T)$ is the energy of the classical trajectory, $\mathbf{q}(t,T)$, going from $\mathbf{q}_0$ to $\mathbf{q}$ in time T, that is, the value of the Hamiltonian H taken at any point on the corresponding phase space trajectory $\mathbf{X}(t,T)=[\mathbf{q}(t,T),\mathbf{p}(t,T)]$.

Writing $T=T_0+\delta T$, the Taylor expansion of $H[\mathbf{X}(t,T_0+\delta T)]$ is easily deduced from the Taylor expansion of $\mathbf{X}(t,T_0+\delta T)$ around the reference trajectory $\mathbf{X}(t,T_0)$ [noted hereafter as $\mathbf{X}^{(0)}(t)$]:

$$\mathbf{X}(t,T_0+\delta T)=\mathbf{X}^{(0)}(t)+\delta T\,\mathbf{X}^{(1)}(t)+\frac{\delta T^2}{2}\mathbf{X}^{(2)}(t) +\frac{\delta T^3}{6}\mathbf{X}^{(3)}(t)+\cdots \tag{28}$$

and from which one obtains the higher derivatives of the classical action $W_l^{(n)}$ at $T=T_0$:

$$\begin{aligned} W_l^{(1)}&=-H[\mathbf{X}^{(0)}(t)],\\ W_l^{(2)}&=-X_i^{(1)}H_i^{(1)},\\ W_l^{(3)}&=-(X_i^{(2)}H_i^{(1)}+X_i^{(1)}X_j^{(1)}H_{ij}^{(2)}),\\ W_l^{(4)}&=-(X_i^{(3)}H_i^{(1)}+3X_i^{(1)}X_j^{(2)}H_{ij}^{(2)}+X_i^{(1)}X_j^{(1)}X_k^{(1)}H_{ijk}^{(3)}), \end{aligned} \tag{29}$$

where all derivatives of H are evaluated at $\mathbf{X}^{(0)}(t)$.

Equations for $\mathbf{X}^{(n)}(t)$ are deduced from Hamilton's equations governing $\mathbf{X}(t,T)$ evolution:

$$\begin{aligned} \dot{X}_i^{(1)}&=\Sigma_{ij}H_{jk}^{(2)}X_k^{(1)},\\ \dot{X}_i^{(2)}&=\Sigma_{ij}H_{jk}^{(2)}X_k^{(2)}+\Sigma_{ij}H_{jkl}^{(3)}X_k^{(1)}X_l^{(1)},\\ \dot{X}_i^{(3)}&=\Sigma_{ij}H_{jk}^{(2)}X_k^{(3)}+3\Sigma_{ij}H_{jkl}^{(3)}X_k^{(1)}X_l^{(2)} +\Sigma_{ij}H_{jklm}^{(4)}X_k^{(1)}X_l^{(1)}X_m^{(1)}, \end{aligned} \tag{30}$$

where again all derivatives of H are evaluated at $\mathbf{X}^{(0)}(t)$. Thus, we are facing three differential sets of the form $\dot{\mathbf{X}}^{(i)}=\Sigma H^{(2)}\mathbf{X}^{(i)}+\Sigma\mathbf{Y}^{(i)}$ (i.e., nonhomogeneous linear differential equations), with the important property that the vector $\mathbf{Y}^{(i)}$ only depends on vectors $\mathbf{X}^{(j)}$ with $j<i$, so that they can be solved one after the other. Solutions of these nonhomogeneous linear differential equations are expressed with the monodromy matrix $M^{(0)}$:

$$\begin{aligned} \mathbf{X}^{(1)}(t)&=M^{(0)}(t)\mathbf{X}^{(1)}(0),\\ \mathbf{X}^{(2)}(t)&=M^{(0)}(t)\mathbf{X}^{(2)}(0)+\mathbf{F}^{(2)}(t),\\ \mathbf{X}^{(3)}(t)&=M^{(0)}(t)\mathbf{X}^{(3)}(0)+\mathbf{F}^{(3)}(t). \end{aligned} \tag{31}$$

Among the $3\times(2f)$-dimensional space of solutions given by preceding expressions, the relevant one is selected by transposing on initial values $\mathbf{X}^{(i)}(0)$ (for $i=1,2,3$) the two boundary conditions

$$\mathbf{q}(0,T_0+\delta T)=\mathbf{q}_0 \quad \text{and} \quad \mathbf{q}(T_0+\delta T,T_0+\delta T)=\mathbf{q}. \tag{32}$$

Introducing position $\mathbf{q}^{(i)}$ and momentum $\mathbf{p}^{(i)}$ parts for vectors $\mathbf{X}^{(i)}$, the Taylor expansion of the preceding equations leads to the following boundary conditions:

$$\mathbf{q}^{(1)}(0)=0 \qquad \mathbf{q}^{(1)}(T_0)=-\dot{\mathbf{q}}^{(0)}(T_0),$$
$$\mathbf{q}^{(2)}(0)=0 \qquad \mathbf{q}^{(2)}(T_0)=-\ddot{\mathbf{q}}^{(0)}(T_0)-2\dot{\mathbf{q}}^{(1)}(T_0),$$
$$\mathbf{q}^{(3)}(0)=0 \quad \text{and} \quad \mathbf{q}^{(3)}(T_0)=-\dddot{\mathbf{q}}^{(0)}(T_0)-3\ddot{\mathbf{q}}^{(1)}(T_0)-3\dot{\mathbf{q}}^{(2)}(T_0). \tag{33}$$

Thus, the initial values $\mathbf{p}^{(i)}(0)$ are implicitly determined by the final values $\mathbf{q}^{(i)}(T_0)$, through the integral expressions (31), which for $\mathbf{X}^{(1)}$ reads

$$\begin{pmatrix}\mathbf{q}^{(1)}(T_0)\\ \mathbf{p}^{(1)}(T_0)\end{pmatrix}=\begin{bmatrix}J_2(T_0) & J_1(T_0)\\ \dot{J}_2(T_0) & \dot{J}_1(T_0)\end{bmatrix}\begin{pmatrix}\mathbf{0}\\ \mathbf{p}^{(1)}(0)\end{pmatrix}, \tag{34}$$

showing thus that $\mathbf{p}^{(1)}(0)=-J_1^{-1}(T_0)\dot{\mathbf{q}}^{(0)}(T_0)$.

Then $\mathbf{F}^{(2)}(T_0)$ and $\mathbf{F}^{(3)}(T_0)$ are easily computed by integrating sets of differential equations obtained from Eq. (30), allowing us to derive $\mathbf{p}^{(2)}(0)$ and $\mathbf{p}^{(3)}(0)$ values from Eq. (31), solving systems similar to Eq. (34):

$$\mathbf{p}^{(2)}(0)=-J_1^{-1}(T_0)[\ddot{\mathbf{q}}^{(0)}(T_0)+2\dot{\mathbf{q}}^{(1)}(T_0)+\mathbf{f}^{(2)}(T_0)],$$
$$\mathbf{p}^{(3)}(0)=-J_1^{-1}(T_0)[\dddot{\mathbf{q}}^{(0)}(T_0)+3\ddot{\mathbf{q}}^{(1)}(T_0)+3\dot{\mathbf{q}}^{(2)}(T_0)+\mathbf{f}^{(3)}(T_0)], \tag{35}$$

where we have introduced the notation $(\mathbf{f}^{(i)},\mathbf{g}^{(i)})$ for vectors $\mathbf{F}^{(i)}$. Quantities like $\dot{\mathbf{q}}^{(1)}(T_0)$, $\ddot{\mathbf{q}}^{(1)}(T_0)$, and $\dot{\mathbf{q}}^{(2)}(T_0)$ can also be expressed in terms of $\mathbf{X}^{(0)}(T_0)$ and its derivatives.

At this point, from the values of the three vectors $\mathbf{X}^{(i)}(T_0)$ and using Eqs. (29) at time T_0, all derivatives $W^{(n)}$ of the classical action can be computed.

We now explain how to compute derivatives of $\det J_1(T)$. More precisely one has to calculate the two coefficients $C_0^{(1)}$ and $C_0^{(2)}$, which are derivatives of $-\ln\sqrt{|\det J_1(T)|}$, so that, using the well-known formula

$$\frac{d}{dT}(\ln|\det J|)=\mathrm{Tr}\left(J^{-1}\frac{dJ}{dT}\right) \tag{36}$$

[J being any (invertible) matrix], expressions of $C_0^{(1)}$ and $C_0^{(2)}$ become

$$C_0^{(1)}=-\frac{1}{2}\mathrm{Tr}\left(J_1^{-1}(T_0)\frac{dJ_1(T_0)}{dT}\right),$$
$$C_0^{(2)}=-\frac{1}{2}\mathrm{Tr}\left(J_1^{-1}(T_0)\frac{d^2J_1(T_0)}{dT^2}-J_1^{-1}(T_0)\frac{dJ_1(T_0)}{dT}J_1^{-1}(T_0)\frac{dJ_1(T_0)}{dT}\right), \tag{37}$$

where $dJ_1(T_0)/dT$ means derivative of $J_1(T_0)$ when changing total time T (and thus the classical orbit), which must not be confused with $\dot{J}_1$ (time derivative of J_1 along a given classical orbit). $J_1(T)$ being the $(f\times f)$ upper right submatrix of the monodromy matrix $M(T)$, $d^nJ_1(T_0)/dT^n$ is also stored at the same position in matrix $d^nM(T_0)/dT^n$, for which we will derive general expressions. For this purpose, we first introduce the explicit notation $M(t,T)$, representing the value of the monodromy matrix at time t along the orbit going from $\mathbf{q}_0$ to $\mathbf{q}$ in time T. Writing $T=T_0+\delta T$, the Taylor expansion of $M(t,T)$ for a given time t reads

$$M(t,T_0+\delta T)=M^{(0)}(t)+\delta T\,M^{(1)}(t)+\frac{\delta T^2}{2}M^{(2)}(t), \tag{38}$$

where $M^{(0)}(t)$ is the monodromy matrix along the reference orbit (i.e., going from $\mathbf{q}_0$ to $\mathbf{q}$ in time T_0). Then $dM(T_0)/dT$ and $d^2M(T_0)/dT^2$ are the Taylor coefficients of monodromy matrix $M(T_0+\delta T,T_0+\delta T)$ and thus have the following expression:

$$\frac{dM(T_0)}{dT}=\dot{M}^{(0)}(T_0)+M^{(1)}(T_0),$$
$$\frac{d^2M(T_0)}{dT^2}=\ddot{M}^{(0)}(T_0)+2\dot{M}^{(1)}(T_0)+M^{(2)}(T_0). \tag{39}$$

Equations governing $M^{(i)}(t)$ evolution are easily deduced from the one for $M(t,T)$:

$$\dot{M}_{ij}^{(1)}=\Sigma_{ik}[H_{kl}^{(2)}M_{lj}^{(1)}+H_{klm}^{(3)}X_m^{(1)}M_{lj}^{(0)}],$$
$$\dot{M}_{ij}^{(2)}=\Sigma_{ik}[H_{kl}^{(2)}M_{lj}^{(2)}+2H_{klm}^{(3)}X_m^{(1)}M_{lj}^{(1)}+H_{klm}^{(3)}X_m^{(2)}M_{lj}^{(0)}+H_{klmn}^{(4)}X_m^{(1)}X_n^{(1)}M_{lj}^{(0)}], \tag{40}$$

with initial conditions $M^{(1)}(0)=M^{(2)}(0)=0$. Obviously these equations are similar to those governing $\mathbf{X}^{(i)}$ evolution, so that $M^{(1)}(T_0)$ and $M^{(2)}(T_0)$ values will be obtained by integrating similar differential sets. Actually, it can be shown that all these sets (for both $\mathbf{X}^{(i)}$ and $M^{(i)}$) can be concatened in only one (larger) set of differential equations, whose integration can be done at once.

Finally, gathering all quantities in Eq. (39), the two matrices $dJ_1(T_0)/dT$ and $d^2J_1(T_0)/dT^2$ are inserted in Eq. (37) thus giving values for $C_0^{(1)}$ and $C_0^{(2)}$, which, along with the values for $W_l^{(n)}$, allow us to compute the numerical value for $C_1^{T\to E}(\mathbf{q},\mathbf{q}_0,T_0)$.

Obviously, the number of equations in the preceding differential sets can be reduced, especially for Hamiltonian separating into kinetic and potential energy, for which $H_{jkl}^{(3)}$ and $H_{jklm}^{(4)}$ coefficients are nonvanishing only when $1\leqslant j,k,l,m\leqslant f$. However, these sets are straightforward to

implement and need only a small amount of CPU time to be solved using any conventional integrator (fourth order Runge-Kutta in the present case).

IV. TRACE OF THE PROPAGATOR $K(T)$

The diagonal elements $K(\mathbf{q}_0,\mathbf{q}_0,T)$ of the propagator are related to classical orbits starting from $\mathbf{q}_0$ and returning to this point after time T, i.e., closed orbits. Summing all these diagonal elements, that is performing the integral $\int d\mathbf{q}_0\, K(\mathbf{q}_0,\mathbf{q}_0,T)$, will select, through another stationary phase approximation, closed orbits for which initial and final momentum are equal: periodic orbits. $\hbar$ corrections to leading order of the semiclassical contribution to $K(T)$ from each periodic orbit can be derived following the same scheme previously used for the propagator itself [1,13].

A. Feynman path integral

Adding the integral over the initial and final positions in Eq. (1) yields [13]

$$K(T)=\int d\mathbf{q}_0\, d\mathbf{q}_1\, d\mathbf{q}_2,\ldots,d\mathbf{q}_{N-1}(2\pi i\hbar\Delta t)^{-Nf/2}\times\exp\left[\frac{i}{\hbar}\sum_{n=0}^{N-1}L\left(\frac{\mathbf{q}_{n+1}-\mathbf{q}_n}{\Delta t},\mathbf{q}_n\right)\Delta t+O(\Delta t)\right] \tag{41}$$

with $\mathbf{q}_N=\mathbf{q}_0$.

The stationary phase approximation around a given periodic orbit $\mathbf{q}_l^{\mathrm{cl}}(t)$ is made explicit when replacing the preceding Nf integral with [13]

$$\int dq_0^{\parallel}\, d\boldsymbol{\xi}_0^{\perp}\, d\boldsymbol{\xi}_1\, d\boldsymbol{\xi}_2,\ldots,d\boldsymbol{\xi}_{N-1} \tag{42}$$

with $\boldsymbol{\xi}_n=\mathbf{q}_n-\mathbf{q}_l^{\mathrm{cl}}(n\Delta t)$. For $n=0$ (i.e., initial position), only deviations perpendicular to the periodic orbit $\boldsymbol{\xi}_0^{\perp}$ have been introduced because the classical action $W_l(\mathbf{q}_0,\mathbf{q}_0,T)$ is constant along the orbit (depicted by $q_0^{\parallel}$). The contribution $K_l(T)$ of this periodic orbit to $K(T)$ then reads [13]

$$K_l(T)=\left(\frac{N}{2\pi i\hbar T}\right)^{Nf/2}\exp\left(\frac{i}{\hbar}W_l\right)\int dq_0^{\parallel}\, d\boldsymbol{\xi}_0^{\perp}\, d\boldsymbol{\xi}_1\times d\boldsymbol{\xi}_2,\ldots,d\boldsymbol{\xi}_{N-1}\exp\left(\frac{i}{2\hbar}W_{,ab}\xi_a\xi_b\right)\times\left[1+\frac{i}{6\hbar}W_{,abc}\xi_a\xi_b\xi_c+\frac{i}{24\hbar}W_{,abcd}\xi_a\xi_b\xi_c\xi_d-\frac{1}{72\hbar^2}W_{,abc}W_{,def}\xi_a\xi_b\xi_c\xi_d\xi_e\xi_f\right], \tag{43}$$

where $\xi_a=\xi_{0i}^{\perp}$ when $a=(0,i)$ and $\xi_a=0$ when $a=(0,0)$. W_l is, in the large N limit, the classical action of the periodic orbit. Full expressions for $W_{,ab}$, $W_{,abc}$, and $W_{,abcd}$ can be found in Ref. [13].

Then, the next step would consist of performing all imaginary Gaussian integrals, leaving out the integral along the orbit. However, in the preceding coordinate transformation (42), there is an hidden subtlety, affecting only $\hbar$ corrections, which probably explains why it is not mentioned in usual textbooks [1,3], where authors are only looking at leading semiclassical amplitudes.

Actually, the problem is that the integral over $q_0^{\parallel}$ corresponds to the length of the classical orbit, only when $\boldsymbol{\xi}_0^{\perp}=\mathbf{0}$; for a nonzero value, it will correspond to integration on a closed curve, slightly displaced from the original trajectory, whose length will thus depend on the $\boldsymbol{\xi}_0^{\perp}$ value. To enlighten this, let us suppose that we have a bidimensional system, for which one periodic orbit is a circle of radius R_0, traveled at constant speed $V_0=2\pi R_0/T$. The coordinate transformation is then easily made using polar coordinates (r,θ):

$$r=R_0-\xi_0^{\perp}. \tag{44}$$

The negative sign appears to preserve orientation. The volume element $dx\,dy$ becomes

$$dx\,dy=r\,d\theta\,dr=(R_0-\xi_0^{\perp})\,d\theta\,d\xi_0^{\perp}, \tag{45}$$

which shows that, in this case, $dq_0^{\parallel}$ is not simply $R_0\,d\theta$, the length on the periodic orbit, but is given by

$$dq_0^{\parallel}=(R_0-\xi_0^{\perp})\,d\theta\neq R_0\,d\theta. \tag{46}$$

This simple example shows actually that the variable $q_0^{\parallel}$ is not independent of $\boldsymbol{\xi}_0^{\perp}$, whereas θ is.

For a general system, the variable that can play the θ role is actually the time t, whose variation domain $[0,T]$ is fixed and then obviously independent of $\boldsymbol{\xi}_0^{\perp}$. Thus one has to generalize the relation $dq_0^{\parallel}=|\dot{\mathbf{q}}^{\mathrm{cl}}|dt_0$, valid only on the periodic orbit. This is done by writing explicitly the coordinate transformation $\mathbf{q}\rightarrow(t_0,\boldsymbol{\xi}_0^{\perp})$:

$$\mathbf{q}=\mathbf{q}^{\mathrm{cl}}(t_0)+\xi_{0i}^{\perp}\mathbf{n}_i(t_0), \tag{47}$$

where $\mathbf{n}_i(t_0)$ are $f-1$ orthogonal unit vectors lying in the plane perpendicular to the periodic orbit at time t_0. The Jacobian of the transformation reads

$$\det\frac{\partial\mathbf{q}}{\partial(t_0,\boldsymbol{\xi}_0^{\perp})}=\det[\dot{\mathbf{q}}^{\mathrm{cl}}+\xi_{0i}^{\perp}\dot{\mathbf{n}}_i,\mathbf{n}_1,\cdots,\mathbf{n}_{f-1}]=|\dot{\mathbf{q}}^{\mathrm{cl}}|-\frac{1}{|\dot{\mathbf{q}}^{\mathrm{cl}}|}\boldsymbol{\xi}_0^{\perp}\cdot\ddot{\mathbf{q}}^{\mathrm{cl}}. \tag{48}$$

Inserting the volume element in Eq. (43), the contribution $K_l(T)$ of the periodic orbit now reads, keeping only terms giving rise to $\hbar$ corrections,

$$K_l(T)=\left(\frac{N}{2\pi i\hbar T}\right)^{Nf/2}\exp\left(\frac{i}{\hbar}W_l\right)\times\int|\dot{\mathbf{q}}^{\rm cl}|dt_0\,d\boldsymbol{\xi}_0^{\perp}d\boldsymbol{\xi}_1d\boldsymbol{\xi}_2,\ldots,d\boldsymbol{\xi}_{N-1}\times\exp\left(\frac{i}{2\hbar}W_{,ab}\xi_a\xi_b\right)\times\left[1+\frac{\xi_{\tilde{d}}V_{,\tilde{d}}}{|\dot{\mathbf{q}}^{\rm cl}|^2}+\frac{i}{6\hbar}W_{,abc}\xi_a\xi_b\xi_c+\frac{i}{24\hbar}W_{,abcd}\xi_a\xi_b\xi_c\xi_d+\frac{i}{6\hbar}\frac{V_{,\tilde{d}}W_{,abc}\xi_{\tilde{d}}\xi_a\xi_b\xi_c}{|\dot{\mathbf{q}}^{\rm cl}|^2}-\frac{1}{72\hbar^2}W_{,abc}W_{,def}\xi_a\xi_b\xi_c\xi_d\xi_e\xi_f\right],\tag{49}$$

where we have seen that $\ddot{\mathbf{q}}^{\rm cl}=-\partial_{\mathbf{q}}V$ and we have introduced the index $\tilde{d}$ for $(0,j)$.

As explained in Ref. [13], the imaginary Gaussian integrals can be expressed in terms of another classical Green's functions $\mathcal{G}(t,t')$, whose boundary conditions are extracted when comparing the detailed expression of $W_{,ab}$ with the discrete version of the Jacobi-Hill operator $\mathcal{D}$, see Eq. (6). Especially, it can be shown that, in the large N limit, they become

$$\begin{aligned}&\mathcal{G}(0,t')=\mathcal{G}(T,t'),\\&\mathcal{P}_{t_0}\mathcal{G}(0,t')=\mathcal{P}_{t_0}\mathcal{G}(T,t')=0,\ \forall\, t'\in[0,T],\\&\mathcal{Q}_{t_0}\dot{\mathcal{G}}(0,t')=\mathcal{Q}_{t_0}\dot{\mathcal{G}}(T,t'),\end{aligned}\tag{50}$$

where we have introduced $\mathcal{P}_{t_0}$ the projector along the periodic orbit at time t_0 and $\mathcal{Q}_{t_0}=\mathbb{1}-\mathcal{P}_{t_0}$. In Ref. [13], only the f^2+f boundary conditions corresponding to the first two lines were given, whereas the f^2-f ones corresponding to the last line were missing.

Performing all imaginary Gaussian integrals and taking the large N limit in Eq. (49), the contribution of the given periodic orbit to the trace of the propagator reads as follows:

$$K_l(T)=K_l^{(0)}(T)\left\{1+i\hbar\frac{1}{T}\int_0^T dt_0C_1(T,t_0)+O(\hbar^2)\right\},\tag{51}$$

$K_l^{(0)}(T)$ being the usual semiclassical leading order [1,13,22]

$$K_l^{(0)}(T)=\frac{1}{\sqrt{2\pi\hbar}}\frac{T}{|\partial_E T\det[m(T)-\mathbb{1}]|^{1/2}}\times\exp\left[\frac{i}{\hbar}W_l(T)-i\frac{\pi}{2}\mu_l+i\,\mathrm{sgn}\,\partial_E T\right],\tag{52}$$

where $W_l(T)$ is the classical action of the periodic orbit and μ_l its Maslov index.

The first $\hbar$ correction $C_1(T)$ to $K_l^{(0)}(T)$ is then obtained by averaging over the time t_0 (i.e., over the full periodic orbit) the coefficient $C_1(T,t_0)$, given by

$$\begin{aligned}C_1(T,t_0)=&\frac{1}{8}\int_0^T dt\,V_{ijkl}^{(4)}(t)\mathcal{G}_{ij}(t,t)\mathcal{G}_{kl}(t,t)\\&+\frac{1}{2}\frac{V_l^{(1)}(t_0)}{|\dot{\mathbf{q}}^{\rm cl}|^2}\int_0^T dt\,V_{ijk}^{(3)}(t)\mathcal{G}_{lk}(0,t)\mathcal{G}_{ij}(t,t)\\&+\frac{1}{24}\int_0^T\int_0^T dt\,dt'\,V_{ijk}^{(3)}(t)V_{lmn}^{(3)}(t')[3\mathcal{G}_{ij}(t,t)\\&\times\mathcal{G}_{kl}(t,t')\mathcal{G}_{mn}(t',t')\\&+2\mathcal{G}_{il}(t,t')\mathcal{G}_{jm}(t,t')\mathcal{G}_{kn}(t,t')],\end{aligned}\tag{53}$$

where t_0 represents thus the position $\mathbf{q}_0$ on the periodic orbit at which boundary conditions (50) on the classical Green's function $\mathcal{G}(t,t')$ are applied. $\mathbf{q}_0$ is also the initial (and final) position on the periodic orbit for classical motions corresponding to times t and t' entered in the preceding expression.

B. Classical Green's function

As in Sec. II B, where expressions for classical Green's functions for the propagator $K(\mathbf{q},\mathbf{q}_0,T)$ where derived, we introduce the $\mathcal{G}_{\pm}(t,t')$ notations and $A_{\pm}(t')$, $B_{\pm}(t')$ matrices. Using all boundary conditions (at times $t=t'$, $t=0$ and $t=T$) gives rise to the following equation:

$$\begin{bmatrix}\mathbb{1}&0\\0&\mathcal{Q}_{t_0}\end{bmatrix}[M(T)-\mathbb{1}_{2f}]\begin{pmatrix}A_-(t')\\B_-(t')\end{pmatrix}=\begin{bmatrix}\mathbb{1}&0\\0&\mathcal{Q}_{t_0}\end{bmatrix}M(T)\begin{pmatrix}-J_1^{\top}(t')\\J_2^{\top}(t')\end{pmatrix}.\tag{54}$$

The preceding set of linear equations, formally written $\mathcal{A}\mathcal{X}=\mathcal{B}$, cannot be solved directly because the $(2f\times 2f)$ matrix $\mathcal{A}$ is obviously singular. More precisely, existence and number of solutions for the system $\mathcal{A}\mathbf{x}=\mathbf{b}$ are determined by the two following properties:

(1) Solutions exists if for all vectors $\mathbf{y}$ such that $\mathcal{A}^{\top}\mathbf{y}=\mathbf{0}$, then $\mathbf{y}\cdot\mathbf{b}=0$.

(2) If the preceding condition is fulfilled, and if $\mathbf{x}$ is a solution, then for all vectors $\mathbf{x}_0$ such that $\mathcal{A}\mathbf{x}_0=\mathbf{0}$, $\mathbf{x}+\mathbf{x}_0$ is also a solution, showing that the dimension of the solution space is that of the nullspace of $\mathcal{A}$.

In the present case, equation $\mathbf{A}^{\top}\mathbf{y}=\mathbf{0}$ leads to either

$$\begin{bmatrix}\mathbb{1}&0\\0&\mathcal{Q}_{t_0}\end{bmatrix}\mathbf{y}=\mathbf{0}\Rightarrow\mathbf{y}\propto\begin{pmatrix}\mathbf{0}\\\dot{\mathbf{q}}(t_0)\end{pmatrix}\tag{55}$$

or

$$[M(T)-\mathbb{1}_{2f}]\tilde{\mathbf{y}}=\mathbf{0}\quad\text{with}\quad\tilde{\mathbf{y}}=\Sigma\begin{bmatrix}\mathbb{1}&0\\0&\mathcal{Q}_{t_0}\end{bmatrix}\mathbf{y}\neq\mathbf{0}.\tag{56}$$

For a generic unstable periodic orbit, the eigenspace associated with the eigenvalue 1 of $M(T)$ (T being the period), is of dimension one and is spanned by the vector parallel to the flow (see the Appendix) $\dot{\mathbf{X}}(t_0)=[\dot{\mathbf{q}}(t_0),\dot{\mathbf{p}}(t_0)]$, so that, in the second case, one gets $\tilde{\mathbf{y}}\propto\dot{\mathbf{X}}(t_0)$ and $\mathbf{y}$ is a solution of

$$\begin{bmatrix} \mathbb{1} & 0 \\ 0 & \mathcal{Q}_{t_0} \end{bmatrix} \mathbf{y} \propto \begin{pmatrix} -\dot{\mathbf{p}}(t_0) \\ \dot{\mathbf{q}}(t_0) \end{pmatrix}, \tag{57}$$

which is impossible unless $\dot{\mathbf{q}}(t_0)=\mathbf{0}$, which, for Hamiltonian separating into kinetic and potential energies, corresponds to a self-retracing periodic orbit, for which a slightly modified approach should be developed [18]. Nevertheless, this case is peculiar, and we will suppose in the rest of the section that $\dot{\mathbf{q}}$ never vanishes along the periodic orbit in consideration.

Thus, the nullspace of $\mathcal{A}^\top$ being one-dimensional and spanned by the vector $[\mathbf{0},\dot{\mathbf{q}}(t_0)]$, Eq. (54) immediately shows that for any column of matrix $\mathcal{B}$, we get $[\mathbf{0},\dot{\mathbf{q}}(t_0)]\cdot\mathcal{B}_i=0$, fulfilling thus the first condition. Denoting $\mathcal{X}_0$ as a solution of Eq. (54), which can be easily obtained using singular value decomposition (SVD) of matrix $\mathcal{A}$, and the nullspace of $M(T)-\mathbb{1}$ being spanned by $\dot{\mathbf{X}}(t_0)$, the general solution of Eq. (54) reads

$$\mathcal{X}=\mathcal{X}_0+[\alpha_1\dot{\mathbf{X}}(t_0),\alpha_2\dot{\mathbf{X}}(t_0),\ldots,\alpha_f\dot{\mathbf{X}}(t_0)], \tag{58}$$

where α_i are unknown real parameters still to be determined. Actually, in Eq. (54) one boundary condition has not been taken into account, namely, that $\mathcal{P}_{t_0}\mathcal{G}_-(0,t')=0$ which, using that the projector $\mathcal{P}_{t_0}$ reads

$$(\mathcal{P}_{t_0})_{ij}=\left(\frac{\dot{\mathbf{q}}(t_0)\dot{\mathbf{q}}^\top(t_0)}{|\dot{\mathbf{q}}(t_0)|^2}\right)_{ij}=\frac{\dot{\mathbf{q}}_i(t_0)\dot{\mathbf{q}}_j(t_0)}{|\dot{\mathbf{q}}(t_0)|^2}, \tag{59}$$

allows us to get α_i values and, from that, the final expression

$$\begin{pmatrix} A_-(t') \\ B_-(t') \end{pmatrix}=\mathcal{X}_0-\frac{1}{|\dot{\mathbf{q}}(t_0)|^2}\begin{bmatrix} \dot{\mathbf{q}}(t_0)\dot{\mathbf{q}}^\top(t_0) & 0 \\ \dot{\mathbf{p}}(t_0)\dot{\mathbf{q}}^\top(t_0) & 0 \end{bmatrix}\mathcal{X}_0, \tag{60}$$

which, of course, is now independent of the particular solution $\mathcal{X}_0$.

Whereas in the case of the propagator $K(\mathbf{q},\mathbf{q}_0,T)$, for which we were able to give an explicit expression (14), the classical Green's function associated with the trace of the propagator $K(T)$ is only defined trough a linear system (54), which nevertheless allows us to obtain its numerical value for any (t,t'). Although it clearly appears that matrix $W_{,ab}$ expression (see Ref. [13]) is symmetric, meaning that the classical Green's function must fulfill the property $\mathcal{G}^\top(t,t')=\mathcal{G}(t',t)$, getting the later directly from Eq. (54) is not obvious. However, in the case of the 2D hydrogen in a magnetic field (see Sec. VI for all details), we have numerically checked that the property holds. For example, in Fig. 2 the four coefficients of classical Green's function $\mathcal{G}(t,t')$ (for $t'/T=0.3$) of the periodic orbit 1234 are plotted with respect to time t. The starting point t_0 on the periodic orbit is depicted by the cross. Actually, we have plotted the coefficient of the rotated matrix $\tilde{\mathcal{G}}(t,t')$, such that its first row corresponds to the direction parallel to the orbit; $\tilde{\mathcal{G}}_{11}(t,t')$ (continuous line) and $\tilde{\mathcal{G}}_{12}(t,t')$ (dotted line) are thus equal to zero for initial $(t=0)$ and final $(t=T)$ points. The other boundary conditions can also be verified in the figure: the dashed line $[\tilde{\mathcal{G}}_{21}(t,t')]$ [respectively, the long dashed line, $\tilde{\mathcal{G}}_{22}(t,t')$] has not only the same value at initial and final time, but also the same slope, which means that $\tilde{\mathcal{G}}_{21}(t,t')$ [respectively, $\tilde{\mathcal{G}}_{22}(t,t')$] and its time derivative fulfill the periodic boundary conditions (50). Finally, for $t=t'$, the off-diagonal coefficients $\tilde{\mathcal{G}}_{12}(t',t')$ (dotted line) and $\tilde{\mathcal{G}}_{21}(t',t')$ (dashed line) are equal, as expected from the symmetry property.

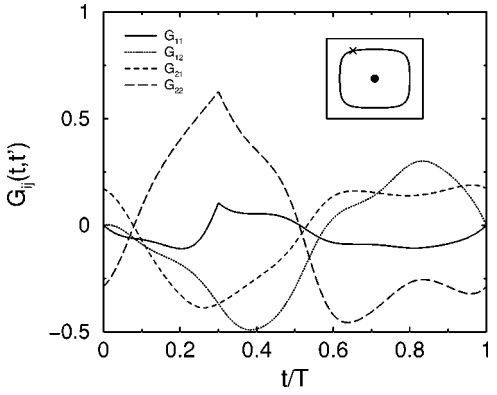

FIG. 2. Example of a classical Green's function $\mathcal{G}(t,t')$ involved in the calculation of the $\hbar$ corrections for the trace of the propagator $K(T)$. It is associated with the periodic orbit $\overline{1234}$ of the 2D hydrogen atom in a magnetic field, whose trajectory in (u,v) coordinates is inserted in the plot (see Sec. VI for all details). The black circle depicts the nucleus, whereas the cross corresponds to the initial and final points on the periodic orbit at which $\mathcal{G}(t,t')$ fulfills the boundary conditions (50). Each curve corresponds to a matrix element $\mathcal{G}_{ij}(t,t')$ plotted with respect to time t, for $t'/T=0.3$. Actually, we have plotted the coefficient of the rotated matrix $\tilde{\mathcal{G}}(t,t')$, such that its first row corresponds to the direction parallel to the orbit; $\tilde{\mathcal{G}}_{11}(t,t')$ (continuous line) and $\tilde{\mathcal{G}}_{12}(t,t')$ (dotted line) are thus equal to zero for initial $(t=0)$ and final $(t=T)$ points. The other boundary conditions can also be verified in the figure; the dashed line $[\tilde{\mathcal{G}}_{21}(t,t')]$ [respectively, the long dashed line, $\tilde{\mathcal{G}}_{22}(t,t')$] has not only the same value at initial and final time, but also the same slope, which means that $\tilde{\mathcal{G}}_{21}(t,t')$ [respectively, $\tilde{\mathcal{G}}_{22}(t,t')$] and its time derivative fulfills the periodic boundary conditions (50). Finally, for $t=t'$, the off-diagonal coefficients $\tilde{\mathcal{G}}_{12}(t',t')$ (dotted line) and $\tilde{\mathcal{G}}_{21}(t',t')$ (dashed line) are equal, as expected from the symmetry property $\mathcal{G}^\top(t,t')=\mathcal{G}(t',t)$.

C. Getting $C_1(T,t_0)$ by integrating a set of first order differential equations

As seen previously (see Sec. II C), we will explain how the numerical value of coefficients $C_1(T,t_0)$ can be obtained

by integrating a set of differential equation, using the standard Runge-Kutta method. There are now four contributions to $C_1(T,t_0)$, namely

$$I_1(T)=\int_0^T dt\, V^{(4)}_{ijkl}(t)\mathcal{G}_{ij}(t,t)\mathcal{G}_{kl}(t,t),$$

$$I_l(T)=\int_0^T dt\, V^{(3)}_{ijk}(t)\mathcal{G}_{lk}(0,t)\mathcal{G}_{ij}(t,t),$$

$$I_2^+(T)=\int_0^T\int_0^T dt\,dt'\, V^{(3)}_{ijk}(t)V^{(3)}_{lmn}(t') \times\mathcal{G}_{ij}(t,t)\mathcal{G}_{kl}(t,t')\mathcal{G}_{mn}(t',t'),$$

$$I_2^-(T)=\int_0^T\int_0^T dt\,dt'\, V^{(3)}_{ijk}(t)V^{(3)}_{lmn}(t') \times\mathcal{G}_{il}(t,t')\mathcal{G}_{jm}(t,t')\mathcal{G}_{kn}(t,t'). \tag{61}$$

The two main difficulties now are that $\mathcal{G}(t,t')$ does not factorize anymore in a product of matrix at time t and a matrix at time t', nor does the symmetric property $\mathcal{G}^\top(t,t')=\mathcal{G}(t',t)$ explicitly appear (even if we have numerically checked that it is fulfilled). Nevertheless, as seen previously, separating $(t>t')$ and $(t<t')$ contributions in $I_2^\pm(T)$ expressions and introducing four quantities $P_p^{(i)}$ for $1\leqslant i\leqslant 4$, allows us to compute I_2^+, by integrating the following set of differential equations from $t=0$ to T [besides equations for $\mathbf{X}(t)$ and $M(t)$]:

$$\dot P_p^{(1)}=A^+_{pl}(t)V^{(3)}_{lmn}(t)\mathcal{G}_{mn}(t,t),\quad \dot P_p^{(3)}=J_{1lp}(t)V^{(3)}_{lmn}(t)\mathcal{G}_{mn}(t,t),$$

$$\dot P_p^{(2)}=B^+_{pl}(t)V^{(3)}_{lmn}(t)\mathcal{G}_{mn}(t,t),\quad \dot P_p^{(4)}=J_{2lp}(t)V^{(3)}_{lmn}(t)\mathcal{G}_{mn}(t,t),$$

$$\begin{aligned}\dot I_2^+ &= V^{(3)}_{ijk}(t)\mathcal{G}_{ij}(t,t)J_{2kp}(t)P_p^{(1)}(t)+V^{(3)}_{ijk}(t)\mathcal{G}_{ij}(t,t)J_{1kp}(t)P_p^{(2)}(t)\\ &\quad+V^{(3)}_{ijk}(t)\mathcal{G}_{ij}(t,t)A^-_{pk}(t)P_p^{(3)}(t)+V^{(3)}_{ijk}(t)\mathcal{G}_{ij}(t,t)B^-_{pk}(t)P_p^{(4)}(t)\end{aligned} \tag{62}$$

with vanishing initial conditions for $P_p^{(i)}$ and I_2^+. For each time step, one must compute matrices A_- and B_- (and from there matrices A_+ and B_+), solving the linear system described in the previous section, using singular value decomposition of matrix $\mathcal{A}$, which, being independent of t, is done before starting the Runge-Kutta integration. Skipping intermediate steps, the differential equations leading to $I_2^-(T)$ computation reads as follow, introducing another eight quantities $Q^{(i)}_{pqr}$:

$$\dot Q^{(1)}_{pqr}=V^{(3)}_{lmn}(t)A^+_{pl}(t)A^+_{qm}(t)A^+_{rn}(t),\quad \dot Q^{(5)}_{pqr}=V^{(3)}_{lmn}(t)J_{2lp}(t)J_{2mq}(t)J_{2nr}(t),$$
$$\dot Q^{(2)}_{pqr}=V^{(3)}_{lmn}(t)A^+_{pl}(t)A^+_{qm}(t)B^+_{rn}(t),\quad \dot Q^{(6)}_{pqr}=V^{(3)}_{lmn}(t)J_{2lp}(t)J_{2mq}(t)J_{1nr}(t),$$
$$\dot Q^{(3)}_{pqr}=V^{(3)}_{lmn}(t)A^+_{pl}(t)B^+_{qm}(t)B^+_{rn}(t),\quad \dot Q^{(7)}_{pqr}=V^{(3)}_{lmn}(t)J_{2lp}(t)J_{1mq}(t)J_{1nr}(t),$$
$$\dot Q^{(4)}_{pqr}=V^{(3)}_{lmn}(t)B^+_{pl}(t)B^+_{qm}(t)B^+_{rn}(t),\quad \dot Q^{(8)}_{pqr}=V^{(3)}_{lmn}(t)J_{1lp}(t)J_{1mq}(t)J_{1nr}(t),$$

$$\begin{aligned}\dot I_2^- &= V^{(3)}_{ijk}(t)J_{2ip}(t)J_{2jq}(t)J_{2kr}(t)Q^{(1)}_{pqr}(t)+3V^{(3)}_{ijk}(t)J_{2ip}(t)J_{2jq}(t)J_{1kr}(t)Q^{(2)}_{pqr}(t)\\ &\quad+3V^{(3)}_{ijk}(t)J_{2ip}(t)J_{1jq}(t)J_{1kr}(t)Q^{(3)}_{pqr}(t)+V^{(3)}_{ijk}(t)J_{1ip}(t)J_{1jq}(t)J_{1kr}(t)Q^{(4)}_{pqr}(t)\\ &\quad+V^{(3)}_{ijk}(t)A^-_{pi}(t)A^-_{qj}(t)A^-_{rk}(t)Q^{(5)}_{pqr}(t)+3V^{(3)}_{ijk}(t)A^-_{pi}(t)A^-_{qj}(t)B^-_{rk}(t)Q^{(6)}_{pqr}(t)\\ &\quad+3V^{(3)}_{ijk}(t)A^-_{pi}(t)B^-_{qj}(t)B^-_{rk}(t)Q^{(7)}_{pqr}(t)+V^{(3)}_{ijk}(t)B^-_{pi}(t)B^-_{qj}(t)B^-_{rk}(t)Q^{(8)}_{pqr}(t)\end{aligned} \tag{63}$$

with vanishing initial conditions for $Q^{(i)}_{pqr}$ and I_2^-. Finally, one must add equations leading to I_l and I_1 computation, namely

$$\dot I_1=V^{(4)}_{ijkl}(t)\mathcal{G}_{ij}(t,t)\mathcal{G}_{kl}(t,t),$$
$$\dot I_l=V^{(3)}_{ijk}(t)A^-_{lk}(t)\mathcal{G}_{ij}(t,t), \tag{64}$$

where we have used $\mathcal{G}_{lk}(0,t)=A^-_{lk}(t)$. Taking into account equations for $\mathbf{X}(t)$ and $M(t)$, this gives rise to a total of $8f^3+4f^2+7f+3$ equations, that is 97 for a 2D system.

In practice, having found a periodic orbit and for a given t_0 along this orbit, the coefficient $C_1(T,t_0)$ is computed in two steps:

(1) achieve the SVD decomposition of the matrix $\mathcal{A}$, appearing on the left-hand side of Eq. (54), and compute the projector matrix appearing on the right-hand side of Eq. (60);

(2) integrate the differential set (63) along the periodic orbit (starting at point depicted by t_0). At any time t, use the preceding SVD decomposition to obtain a solution $\mathcal{X}_0$ and the projector matrix to get the true solution $[A_-(t),B_-(t)]$ and thus $[A_+(t),B_+(t)]$, using Eq. (60).

Finally, the coefficient $C_1(T,t_0)$, being a smooth function of t_0, the average over time t_0, leading to the $\hbar$ correction term $C_1(T)$, can be handled by any conventional integrator.

V. TRACE OF THE GREEN'S FUNCTION $G(E)$

Steps leading to the semiclassical contribution $G_l(E)$ from a given periodic orbit to the trace of the Green's function $G(E)$ are identical to those giving the $G_l(\mathbf{q},\mathbf{q}_0,E)$ expression, so that $G_l(E)$ reads

$$G_l(E)=\frac{1}{i\hbar}\frac{T_0}{|\det[m(T_0)-\mathbb{1}]|^{1/2}}\exp\left[\frac{i}{\hbar}S_l(E)-i\frac{\pi}{2}\mu_l\right]\times\{1+i\hbar[C_1(T_0)+C_1^{T\to E}(T_0)]+O(\hbar^2)\}, \quad (65)$$

where $C_1^{T\to E}(T)$ is given by

$$C_1^{T\to E}(T_0)=\frac{1}{2W_l^{(2)}}[(C_0^{(1)})^2+C_0^{(2)}]-\frac{W_l^{(3)}C_0^{(1)}}{2(W_l^{(2)})^2}-\frac{W_l^{(4)}}{8(W_l^{(2)})^2}+\frac{5}{24}\frac{(W_l^{(3)})^2}{(W_l^{(2)})^3}. \quad (66)$$

$W_l^{(i)}$ (respectively, $C_0^{(i)}$) are the Taylor coefficients of the $W_l(T)$ [respectively, $C_0(T)$] expansion around T_0.

Computation of $W_l^{(i)}$ is much the same as in the Green's function case, because the functional relation

$$\frac{\partial W_l(T)}{\partial T}=-E(T) \quad (67)$$

still holds for a given periodic orbit, $E(T)$ being its energy as function of its period, which is still given by the value of the Hamiltonian H taken at any point on the corresponding phase space trajectory $\mathbf{X}(t,T)=[\mathbf{q}(t,T),\mathbf{p}(t,T)]$. Thus, the Taylor expansion of $\mathbf{X}(t,T)$ around the periodic orbit $\mathbf{X}(t,T_0)$, will lead to the same expressions for $W_l^{(i)}$ coefficients [Eq. (29)] and for $\mathbf{X}^{(n)}(t)$ equations [Eq. (30)]. The only differences with the preceding section arise from the boundary conditions fulfilled by $\mathbf{X}^{(n)}(t)$, deduced from the equation $\mathbf{X}(0,T)=\mathbf{X}(T,T)$, i.e., $\mathbf{X}(t,T)$ is a periodic orbit of period T. The Taylor expansion of this relation leads to the following conditions:

$$\begin{aligned}\mathbf{X}^{(1)}(0)&=\mathbf{X}^{(1)}(T_0)+\dot{\mathbf{X}}^{(0)}(T_0),\\ \mathbf{X}^{(2)}(0)&=\mathbf{X}^{(2)}(T_0)+\ddot{\mathbf{X}}^{(0)}(T_0)+2\dot{\mathbf{X}}^{(1)}(T_0),\\ \mathbf{X}^{(3)}(0)&=\mathbf{X}^{(3)}(T_0)+\dddot{\mathbf{X}}^{(0)}(T_0)+3\ddot{\mathbf{X}}^{(1)}(T_0)+3\dot{\mathbf{X}}^{(2)}(T_0).\end{aligned} \quad (68)$$

Solutions of the differential set (30) still have the following formal expressions (31), which, inserted in the boundary conditions (68), leads to equations on $\mathbf{X}^{(i)}(0)$ only:

$$\begin{aligned}[\mathbb{1}-M(T_0)]\mathbf{X}^{(1)}(0)&=\dot{\mathbf{X}}^{(0)}(T_0),\\ [\mathbb{1}-M(T_0)]\mathbf{X}^{(2)}(0)&=\ddot{\mathbf{X}}^{(0)}(T_0)+2\dot{\mathbf{X}}^{(1)}(T_0)+\mathbf{F}^{(2)}(T_0),\\ [\mathbb{1}-M(T_0)]\mathbf{X}^{(3)}(0)&=\dddot{\mathbf{X}}^{(0)}(T_0)+3\ddot{\mathbf{X}}^{(1)}(T_0)+3\ddot{\mathbf{X}}^{(2)}(T_0)+\mathbf{F}^{(3)}(T_0).\end{aligned} \quad (69)$$

The matrix $\mathbb{1}-M(T_0)$ being singular, solving the preceding linear equations need additional discussion, which, for simplicity, will focus on $\mathbf{X}^{(1)}(0)$ only. First, the nullspace of $\mathbb{1}-M(T_0)^\top$ is spanned by $\Sigma\dot{\mathbf{X}}^{(0)}(T_0)$, which is obviously orthogonal to $\dot{\mathbf{X}}^{(0)}(T_0)$, the right-hand side of the equation for $\mathbf{X}^{(1)}(0)$, thus showing that this equation admits solutions. Then, the nullspace of $\mathbb{1}-M(T_0)$ being spanned by $\dot{\mathbf{X}}^{(0)}(T_0)$, the whole set of solutions reads

$$\mathbf{X}^{(1)}(0)=\mathbf{X}_0^{(1)}(0)+\alpha\dot{\mathbf{X}}^{(0)}(T_0), \quad (70)$$

where $\mathbf{X}_0^{(1)}(0)$ is a particular solution of the equation. Actually, the term $\alpha\dot{\mathbf{X}}^{(0)}(T_0)$ corresponds to a displacement of the initial conditions along the flow, which, of course, gives back the same periodic orbit (at first order in $T-T_0$). We thus expect that this term has a vanishing contribution to $W_l^{(2)}$, which is easily verified when inserting the general solution in the $W_l^{(2)}$ expression (taken at time $t=T_0$):

$$\begin{aligned}W_l^{(2)}&=-[\mathbf{X}_0^{(1)}(0)-\dot{\mathbf{X}}^{(0)}(T_0)+\alpha\dot{\mathbf{X}}^{(0)}(T_0)]\cdot\boldsymbol{\nabla}H[\mathbf{X}^{(0)}(T_0)]\\ &=-\mathbf{X}_0^{(1)}(0)\cdot\boldsymbol{\nabla}H[\mathbf{X}^{(0)}(T_0)]\end{aligned} \quad (71)$$

because of the Hamilton's equations $\dot{\mathbf{X}}^{(0)}(T_0)=\Sigma\boldsymbol{\nabla}H[\mathbf{X}^{(0)}(T_0)]$.

These two properties also hold in the cases of $\mathbf{X}^{(2)}(0)$ and $\mathbf{X}^{(3)}(0)$, but are slightly more complicated to establish because the right-hand sides of the equations involve $\mathbf{F}^{(i)}(T_0)$ and derivatives of $\mathbf{X}^{(i)}(T_0)$.

Thus, integrating the same differential sets that were used for $G(\mathbf{q},\mathbf{q}_0,E)$, one is able to compute the first four derivatives of the action, $W_l^{(i)}$, with respect to the period.

Starting from the $C_0^{(0)}(T)$ expression

$$C_0^{(0)}(T)=\ln T-\tfrac{1}{2}\ln|\partial_E T|-\tfrac{1}{2}\ln|\det[m(T)-\mathbb{1}]| \quad (72)$$

and using the fact that $\partial_E T=1/\partial_T E=-1/\partial_T^2 W_l$, one obtains

$$C_0^{(1)}(T_0)=\frac{1}{T_0}+\frac{1}{2}\frac{W_l^{(3)}}{W_l^{(2)}}-\frac{1}{2}\frac{d}{dT}\ln|\det[m(T)-\mathbb{1}]|,$$
$$C_0^{(2)}(T_0)=-\frac{1}{T_0^2}+\frac{1}{2}\frac{W_l^{(4)}}{W_l^{(2)}}-\frac{1}{2}\left(\frac{W_l^{(3)}}{W_l^{(2)}}\right)^2-\frac{1}{2}\frac{d^2}{dT^2}\ln|\det[m(T)-\mathbb{1}]|, \tag{73}$$

which means that one is left with the calculation of derivatives of $\ln|\det[m(T)-\mathbb{1}]|$ with respect to the period T. As shown in the Appendix, $\det[m(T)-\mathbb{1}]$ is given by the determinant of the $2f\times 2f$ matrix $N(T)$ defined as follows:

$$N(T)=M(T)-[\mathbb{1}-\mathcal{P}_\parallel(T)-\mathcal{P}_\perp(T)], \tag{74}$$

where we have introduced $\mathcal{P}_\parallel(T)$ [respectively, $\mathcal{P}_\perp(T)$] the projector on the direction parallel to the flow (respectively, perpendicular to the energy shell), more precisely, the $\mathcal{P}_\parallel(T)$ and $\mathcal{P}_\perp(T)$ expressions are

$$\mathcal{P}_\parallel=\mathbf{e}_\parallel\cdot\mathbf{e}_\parallel^\top \quad \text{and} \quad \mathcal{P}_\perp=\mathbf{e}_\perp\cdot\mathbf{e}_\perp^\top=-\Sigma\mathcal{P}_\parallel\Sigma, \tag{75}$$

where $\mathbf{e}_\parallel$ is the unit vector tangent to the flow at initial (and thus final) time and $\mathbf{e}_\perp=\Sigma\mathbf{e}_\parallel$. Now, using again formula (36), derivatives of $\det[m(T)-\mathbb{1}]$ with respect to the period read

$$\frac{d}{dT}\{\det[m(T)-\mathbb{1}]\}=\mathrm{Tr}\left(N(T_0)^{-1}\frac{dN(T_0)}{dT}\right),$$
$$\frac{d^2}{dT^2}\{\det[m(T)-\mathbb{1}]\}=\mathrm{Tr}\left(N^{-1}(T_0)\frac{d^2N(T_0)}{dT^2}-N(T_0)^{-1}\frac{dN(T_0)}{dT}N(T_0)^{-1}\frac{dN(T_0)}{dT}\right) \tag{76}$$

with

$$\frac{dN(T_0)}{dT}=\frac{dM(T_0)}{dT}+\frac{d\mathcal{P}_\parallel(T_0)}{dT}-\Sigma\frac{d\mathcal{P}_\parallel(T_0)}{dT}\Sigma,$$
$$\frac{d^2N(T_0)}{dT^2}=\frac{d^2M(T_0)}{dT^2}+\frac{d^2\mathcal{P}_\parallel(T_0)}{dT^2}-\Sigma\frac{d^2\mathcal{P}_\parallel(T_0)}{dT^2}\Sigma. \tag{77}$$

As seen previously (Sec. III B), $dM(T_0)/dT$ and $d^2M(T_0)/dT^2$ are expressed in terms of the coefficients $M^{(i)}(t)$ of the Taylor expansion of the monodromy matrix $M(t,T)$ [associated with the periodic orbit $\mathbf{X}(t,T)$ of period T] around the periodic orbit $\mathbf{X}^{(0)}(t)$ of period T_0, see Eq. (39).

Inserting the Taylor expansion of $\dot{\mathbf{X}}(T)$ around T_0 in the $\mathcal{P}_\parallel(T)$ expression, namely,

$$\mathcal{P}_\parallel(T)=\frac{1}{\|\dot{\mathbf{X}}(T)\|^2}\dot{\mathbf{X}}(T)\cdot\dot{\mathbf{X}}(T)^\top, \tag{78}$$

one obtains the derivatives of $\mathcal{P}_\parallel(T)$ with respect to T:

$$\frac{d\mathcal{P}_\parallel(T_0)}{dT}=\frac{1}{\|\dot{\mathbf{X}}^{(0)}\|^2}(\dot{\mathbf{X}}^{(1)}\cdot\dot{\mathbf{X}}^{(0)^\top}+\dot{\mathbf{X}}^{(0)}\cdot\dot{\mathbf{X}}^{(1)^\top})-2\frac{\dot{\mathbf{X}}^{(0)^\top}\cdot\dot{\mathbf{X}}^{(1)}}{\|\dot{\mathbf{X}}^{(0)}\|^2}\mathcal{P}_\parallel(T_0),$$
$$\frac{d^2\mathcal{P}_\parallel(T_0)}{dT^2}=\frac{1}{\|\dot{\mathbf{X}}^{(0)}\|^2}(\dot{\mathbf{X}}^{(2)}\cdot\dot{\mathbf{X}}^{(0)^\top}+\dot{\mathbf{X}}^{(0)}\cdot\dot{\mathbf{X}}^{(2)^\top}+2\dot{\mathbf{X}}^{(1)}\cdot\dot{\mathbf{X}}^{(1)^\top})+\left(8\frac{(\dot{\mathbf{X}}^{(0)^\top}\cdot\dot{\mathbf{X}}^{(1)})^2}{\|\dot{\mathbf{X}}^{(0)}\|^4}-2\frac{\dot{\mathbf{X}}^{(0)^\top}\cdot\dot{\mathbf{X}}^{(2)}}{\|\dot{\mathbf{X}}^{(0)}\|^2}-2\frac{\dot{\mathbf{X}}^{(1)^\top}\cdot\dot{\mathbf{X}}^{(1)}}{\|\dot{\mathbf{X}}^{(0)}\|^2}\right)\mathcal{P}_\parallel(T_0)$$
$$-4\frac{\dot{\mathbf{X}}^{(0)^\top}\cdot\dot{\mathbf{X}}^{(1)}}{\|\dot{\mathbf{X}}^{(0)}\|^4}(\dot{\mathbf{X}}^{(1)}\cdot\dot{\mathbf{X}}^{(0)^\top}+\dot{\mathbf{X}}^{(0)}\cdot\dot{\mathbf{X}}^{(1)^\top}), \tag{79}$$

where all $\dot{\mathbf{X}}^{(i)}$ are evaluated at time $t=0$.

Gathering the preceding expressions into Eq. (76) allows us to compute $\ln\det[m(T)-1]$ derivatives, which, inserted together with derivatives of the action, in Eq. (73) gives the numerical values for $C_0^{(1)}(T_0)$ and $C_0^{(2)}(T_0)$, which finally leads to the additional $\hbar$ correction $C_1^{T\to E}(T_0)$.

VI. APPLICATION TO THE 2D HYDROGEN ATOM IN A MAGNETIC FIELD

The hydrogen atom is one example of a quantum system whose classical counterpart depicts a chaotic behavior and has been widely studied (see, e.g., Ref. [4] for a complete review). It has now become a very useful tool for testing new ideas and tools in the quantum chaos area, both on the semiclassical [20,23] or universality [24] points of view, especially because computing very highly excited states has become a standard task on a regular workstation, allowing the semiclassical regime to be reached easily. Even if one would have preferred to work with the real hydrogen atom (i.e., the three-dimensional one), in this paper we will focus on the two dimensional hydrogen atom in a magnetic field, because taking into account invariance by rotation around the magnetic field, gives rise to centrifugal terms in the Hamiltonian (typically $\mathbf{L}^2\hbar^2/2r^2$) which would also contribute to $\hbar$ corrections and would need a study on its own. One must also notice that, even if the classical dynamics are identical for both cases, the fact that the magnetic field axis is no longer a rotation axis in the 2D case gives rise to slight modifications in the Maslov indices [18,23,25].

A. Quantum and Classical Properties

In atomic units the Hamiltonian of the 2D hydrogen in a magnetic field reads

$$H=\frac{1}{2}\mathbf{p}^2-\frac{1}{\sqrt{x^2+y^2}}+\frac{1}{8}\gamma^2y^2, \tag{80}$$

where $\gamma=B/B_0$, with $B_0=2.35\times10^5T$. The classical counterpart of this Hamiltonian has a scaling property, that is, if we define new variables by

$$\begin{aligned}\tilde{\mathbf{r}}&=\gamma^{2/3}\mathbf{r},\\ \tilde{\mathbf{p}}&=\gamma^{-1/3}\mathbf{p},\\ \tilde{t}&=\gamma t,\end{aligned} \tag{81}$$

we obtain a new Hamiltonian $\tilde{H}$ given by

$$\tilde{H}=\gamma^{-2/3}H=\frac{\tilde{\mathbf{p}}^2}{2}-\frac{1}{\sqrt{\tilde{x}^2+\tilde{y}^2}}+\frac{\tilde{y}^2}{8}, \tag{82}$$

which does not depend on γ anymore. The classical dynamics of this Hamiltonian is entirely fixed by the scaled energy ϵ given by

$$\epsilon=\gamma^{-2/3}E. \tag{83}$$

All properties of the classical trajectories of the original Hamiltonian can be deduced from the scaled dynamics using the scaling transformation (81). From the quantum point of view, this scaling introduces an effective $\hbar$ value, which is easily seen on the scaled Schrödinger equation, $\tilde{H}\psi=\epsilon\psi$, for a fixed scaled energy ϵ:

$$\left[-\frac{\gamma^{2/3}}{2}\Delta_{\tilde{\mathbf{r}}}-\frac{1}{\sqrt{\tilde{x}^2+\tilde{y}^2}}+\frac{\tilde{y}^2}{8}\right]\psi=\epsilon\psi. \tag{84}$$

Thus, the effective $\hbar$ is given by $\gamma^{1/3}$ and so at a fixed value of the scaled energy ϵ, the semiclassical limit is obtained when γ tends to 0.

The singularity in the classical equations of motion due to the divergence of the Coulomb potential at $\mathbf{r}=\mathbf{0}$ is regularized using the semiparabolic coordinates ($u=\sqrt{\tilde{r}+\tilde{x}}, v=\sqrt{\tilde{r}-\tilde{x}}$), giving rise to the following effective classical Hamiltonian [4,26]:

$$\mathcal{H}=\tfrac{1}{2}p_u^2+\tfrac{1}{2}p_v^2-\epsilon(u^2+v^2)+\tfrac{1}{8}u^2v^2(u^2+v^2), \tag{85}$$

the trajectories corresponding to the original problem are obtained when fixing total energy $\mathcal{H}=2$. The associated quantum Hamiltonian reads

$$\begin{aligned}\hat{\mathcal{H}}(\hbar)=&-\frac{\hbar^2}{2}\left(\frac{\partial^2}{\partial u^2}+\frac{\partial^2}{\partial v^2}\right)\\ &-\epsilon(u^2+v^2)+\frac{1}{8}u^2v^2(u^2+v^2),\end{aligned} \tag{86}$$

which separates into kinetic and potential energy, so that the semiclassical formula derived in the preceding sections applied to the associated quantum Green's function $G(z,\hbar)$, the hydrogen in a magnetic field being recovered for $z=2$ (actually $z/2$ corresponds to the nucleus charge)

$$G(z,\hbar)=\frac{1}{z-\hat{\mathcal{H}}(\hbar)}=\sum_\tau\frac{|\tau,\hbar\rangle\langle\tau,\hbar|}{z-\lambda_\tau(\hbar)}, \tag{87}$$

where $|\tau,\hbar\rangle$ is an (normalized) eigenvector of $\hat{\mathcal{H}}(\hbar)$ for the eigenenergy $\lambda_\tau(\hbar)$, τ representing the set of quantum labels, i.e., level number and symmetry properties (see below), describing $|\tau,\hbar\rangle$. The matrix element $\langle\mathbf{q}|G(z,\hbar)|\mathbf{q}_0\rangle$, where $\mathbf{q}=(u,v)$ then reads

$$\langle\mathbf{q}|G(z,\hbar)|\mathbf{q}_0\rangle=\sum_\tau\psi_{\tau,\hbar}(\mathbf{q})\psi_{\tau,\hbar}(\mathbf{q}_0)\frac{1}{z-\lambda_\tau(\hbar)}, \tag{88}$$

where $\psi_{\tau,\hbar}(\mathbf{q})=\langle\mathbf{q}|\tau,\hbar\rangle$ has been supposed to be real, with $\hat{\mathcal{H}}(\hbar)$ being invariant under $\mathbf{p}\to-\mathbf{p}$. Taking $z=\lambda$ on the real axis, the imaginary part of $\langle\mathbf{q}|G(z,\hbar)|\mathbf{q}_0\rangle$, becomes

$$-\frac{1}{\pi}\mathrm{Im}\langle\mathbf{q}|G(\lambda,\hbar)|\mathbf{q}_0\rangle=\sum_\tau\psi_{\tau,\hbar}(\mathbf{q})\psi_{\tau,\hbar}(\mathbf{q}_0)\,\delta[\lambda-\lambda_\tau(\hbar)] \tag{89}$$

to which any classical path going from $\mathbf{q}$ to $\mathbf{q}_0$ at energy λ, gives the following contribution [see Eq. (25)]:

$$-\frac{1}{\pi}\mathrm{Im}\langle\mathbf{q}|G(\lambda,\hbar)|\mathbf{q}_0\rangle_l=\frac{2}{(2\pi\hbar)^{3/2}}\mathcal{A}_l\left\{\cos\left(\frac{1}{\hbar}S_l+\phi_l\right)-\hbar\mathcal{C}_l\sin\left(\frac{1}{\hbar}S_l+\phi_l\right)\right\} \tag{90}$$

provided it is far enough from any bifurcation and that $\mathbf{q}$ and $\mathbf{q}_0$ are not conjugate points for this trajectory. Amplitudes and phases being defined by

$$\begin{aligned}\mathcal{A}_l&=\frac{1}{|W_l^{(2)}\det J_1(T_0)|^{1/2}},\\ S_l&=S(\mathbf{q},\mathbf{q}_0,\lambda),\\ \phi_l&=-\frac{\pi}{2}\left(\tilde{\nu}_l+\frac{1}{2}\right),\\ \mathcal{C}_l&=C_1(\mathbf{q},\mathbf{q}_0,T_0)+C_1^{T\to E}(\mathbf{q},\mathbf{q}_0,T_0).\end{aligned} \tag{91}$$

Neglecting $\hbar$ corrections in Eq. (90), the Fourier transform with respect to the variable $\zeta=1/\hbar$ of the following function:

$$\begin{aligned}g_0(\zeta)&=\frac{(2\pi)^{3/2}}{2\zeta^{3/2}}\times-\frac{1}{\pi}\mathrm{Im}\langle\mathbf{q}|G(\lambda,\zeta)|\mathbf{q}_0\rangle\\&=\frac{(2\pi)^{3/2}}{2}\sum_\tau\ \psi_{\tau,\zeta}(\mathbf{q})\psi_{\tau,\zeta}(\mathbf{q}_0)\zeta^{-3/2}\delta[\lambda-\lambda_\tau(\zeta)]\end{aligned} \tag{92}$$

will depict peaks at the classical actions $S_l/2\pi$, with complex amplitude $\mathcal{A}_l\exp i\phi_l/2$, which has been extensively used to compare the exact quantum Green's function with its semiclassical estimation at the leading order in $\hbar$. In the same way, the Fourier transform of the following function:

$$g_1(\zeta)=-\frac{(2\pi)^{3/2}}{2}\sum_\tau\ \psi_{\tau,\zeta}(\mathbf{q})\psi_{\tau,\zeta}(\mathbf{q}_0)\zeta^{-1/2}\times\delta[\lambda-\lambda_\tau(\zeta)]-\zeta\sum_l\ \mathcal{A}_l\cos(\zeta S_l+\phi_l) \tag{93}$$

will also depict peaks at the classical actions $S_l/2\pi$, whose complex amplitude, given by

$$\frac{1}{2i}\mathcal{A}_l\mathcal{C}_l\exp i\phi_l \tag{94}$$

allows us to extract the numerical value of the $\hbar$ correction C_l.

The energy λ being fixed, the $\delta[\lambda-\lambda_\tau(\zeta)]$ function selects the values $\zeta_\tau(\lambda)$ of ζ for which λ is an eigenvalue, transforming Eqs. (92) and (93) into

$$\begin{aligned}g_0(\zeta)&=\frac{(2\pi)^{3/2}}{4}\sum_\tau\ \frac{\psi_{\tau,\zeta}(\mathbf{q})\psi_{\tau,\zeta}(\mathbf{q}_0)}{\langle\tau,\zeta|\mathbf{p}^2/2|\tau,\zeta\rangle}\zeta^{3/2}\delta[\zeta-\zeta_\tau(\lambda)],\\ g_1(\zeta)&=-\frac{(2\pi)^{3/2}}{4}\sum_\tau\ \frac{\psi_{\tau,\zeta}(\mathbf{q})\psi_{\tau,\zeta}(\mathbf{q}_0)}{\langle\tau,\zeta|\mathbf{p}^2/2|\tau,\zeta\rangle}\\&\quad\times\zeta^{5/2}\delta[\zeta-\zeta_\tau(\lambda)]-\zeta\sum_l\ \mathcal{A}_l\cos(\zeta S_l+\phi_l).\end{aligned} \tag{95}$$

Moving to the case of the trace of the Green's function, the preceding relations (89) and (90) become

$$-\frac{1}{\pi}\mathrm{Im\,Tr}\,G(\lambda,\hbar)=\sum_\tau\ \delta[\lambda-\lambda_\tau(\hbar)] \tag{96}$$

and, see Eq. (65):

$$-\frac{1}{\pi}\mathrm{Im\,Tr}\,G(\lambda,\hbar)_l=-\frac{1}{\pi\hbar}\mathcal{A}_l^{\mathrm{tr}}\left\{\cos\left(\frac{1}{\hbar}S_l^{\mathrm{tr}}+\phi_l^{\mathrm{tr}}\right)-\hbar\mathcal{C}_l^{\mathrm{tr}}\sin\left(\frac{1}{\hbar}S_l^{\mathrm{tr}}+\phi_l^{\mathrm{tr}}\right)\right\}, \tag{97}$$

where S_l^{tr} is the action of the periodic orbit and

$$\begin{aligned}\mathcal{A}_l^{\mathrm{tr}}&=\frac{T_0}{|\det[m(T_0)-\mathbb{1}]|^{1/2}},\\ \phi_l^{\mathrm{tr}}&=-\frac{\pi}{2}\mu_l,\\ \mathcal{C}_l^{\mathrm{tr}}&=C_1(T_0)+C_1^{T\to E}(T_0),\end{aligned} \tag{98}$$

so that the classical quantities S_l^{tr}, $\mathcal{A}_l^{\mathrm{tr}}$, and the $\hbar$ correction $\mathcal{C}_l^{\mathrm{tr}}$ can be obtained by taking the Fourier transform of the following expressions with respect to the variable ζ:

$$\begin{aligned}g_0^{\mathrm{tr}}(\zeta)&=\frac{\pi}{2}\sum_\tau\ \frac{1}{\langle\tau,\zeta|\mathbf{p}^2/2|\tau,\zeta\rangle}\zeta^2\delta[\zeta-\zeta_\tau(\lambda)],\\ g_1^{\mathrm{tr}}(\zeta)&=-\frac{\pi}{2}\sum_\tau\ \frac{1}{\langle\tau,\zeta|\mathbf{p}^2/2|\tau,\zeta\rangle}\zeta^3\delta[\zeta-\zeta_\tau(\lambda)]\\&\quad-\zeta\sum_l\ \mathcal{A}_l^{\mathrm{tr}}\cos(\zeta S_l^{\mathrm{tr}}+\phi_l^{\mathrm{tr}}).\end{aligned} \tag{99}$$

B. Computing quantum quantities

Focusing on the $\lambda=2$ value, the 2D hydrogen in a magnetic field case, one has to find effective $\hbar$ values for which 2 is an eigenvalue of the Schrödinger equation $\hat{\mathcal{H}}(\hbar)\psi(u,v)=2\psi(u,v)$, which is conveniently written as follows:

$$\left[2+\epsilon(u^2+v^2)-\frac{1}{8}u^2v^2(u^2+v^2)\right]\psi(u,v)$$
$$=\hbar^2\left[-\frac{1}{2}\left(\frac{\partial^2}{\partial u^2}+\frac{\partial^2}{\partial v^2}\right)\right]\psi(u,v) \quad (100)$$

such that $\sigma=\hbar^2$ appears to be a solution of a generalized eigenvalue problem $(A-\sigma B)\psi=0$, with

$$A=2+\epsilon(u^2+v^2)-\frac{1}{8}u^2v^2(u^2+v^2),$$
$$B=-\frac{1}{2}\left(\frac{\partial^2}{\partial u^2}+\frac{\partial^2}{\partial v^2}\right). \quad (101)$$

The preceding operators A, B, and thus $\hat{\mathcal{H}}(\hbar)$ are invariant under all transformations belonging to the symmetry group C_{4v}, leading to four nondegenerate series of energy levels, labeled EEE, EEO, OOE, and OOO according to Ref. [27] and a twofold degenerate series EO and OE, where E means even and O means odd, the first two letters referring to the $u\to -u$ and $v\to -v$ symmetries, the third letter to $u\leftrightarrow v$. Actually, because of the definition of the semiparabolic coordinates (u,v), only eigenvectors invariant under the parity symmetry $\psi(-u,-v)=\psi(u,v)$ correspond to eigenvectors of the 2D hydrogen in magnetic field, allowing us, in principle, to drop the OE and EO series [4,26]. However, from the semiclassical point of view, one would have to extend all preceding sections to symmetry-projected propagator and Green's function [28], and thus to take into account symmetry properties of the classical Green's function, which is beyond the scope of this paper. For this reason, we also include the OE and EO series in the remainder of this paper.

Finally, eigenvalues and eigenvectors are obtained by solving the matrix representation of the generalized eigenvalue problem $(A-\sigma B)\psi=0$ in sturmian bases (one for each symmetry class) [4], using the Lanczos algorithm. Typically, we have computed effective $\hbar$ values ranging from 0 to 124, which for scaled energy $\epsilon=-0.1$ corresponds to roughly 61 000 eigenvalues in total. One must notice that the generalized eigenvectors $|\widetilde{\tau,\hbar}\rangle$, for a fixed $\hbar$ value, are actually orthogonal for the scalar product defined by operator $B=\mathbf{p}^2/2$:

$$\langle\widetilde{\tau,\hbar}|\frac{\mathbf{p}^2}{2}|\widetilde{\tau',\hbar}\rangle=\delta_{\tau\tau'} \quad (102)$$

so that the $|\widetilde{\tau,\hbar}\rangle$ and $|\tau,\hbar\rangle$ relations read

$$|\tau,\hbar\rangle=\frac{1}{\sqrt{\langle\widetilde{\tau,\hbar}|\widetilde{\tau,\hbar}\rangle}}|\widetilde{\tau,\hbar}\rangle,$$
$$|\widetilde{\tau,\hbar}\rangle=\frac{1}{\sqrt{\langle\tau,\hbar|B|\tau,\hbar\rangle}}|\tau,\hbar\rangle, \quad (103)$$

giving rise to $g_{0,1}(\zeta)$ (95) and $g_{0,1}^{\mathrm{tr}}(\zeta)$ (99) expressions in terms of the computed eigenvectors:

$$g_0(\zeta)=\frac{(2\pi)^{3/2}}{4}\sum_\tau \tilde{\psi}_{\tau,\zeta}(\mathbf{q})\tilde{\psi}_{\tau,\zeta}(\mathbf{q}_0)\zeta^{3/2}\delta[\zeta-\zeta_\tau(2)],$$
$$g_1(\zeta)=-\frac{(2\pi)^{3/2}}{4}\sum_\tau \tilde{\psi}_{\tau,\zeta}(\mathbf{q})\tilde{\psi}_{\tau,\zeta}(\mathbf{q}_0)\zeta^{5/2}\delta[\zeta-\zeta_\tau(2)]-\zeta\sum_l \mathcal{A}_l\cos(\zeta S_l+\phi_l),$$
$$g_0^{\mathrm{tr}}(\zeta)=\frac{\pi}{2}\sum_\tau \langle\widetilde{\tau,\zeta}|\widetilde{\tau,\zeta}\rangle\,\zeta^2\delta[\zeta-\zeta_\tau(2)],$$
$$g_1^{\mathrm{tr}}(\zeta)=-\frac{\pi}{2}\sum_\tau \langle\widetilde{\tau,\zeta}|\widetilde{\tau,\zeta}\rangle\,\zeta^3\delta[\zeta-\zeta_\tau(2)]-\zeta\sum_l \mathcal{A}_l^{\mathrm{tr}}\cos(\zeta S_l^{\mathrm{tr}}+\phi_l^{\mathrm{tr}}). \quad (104)$$

As explained previously, the Fourier transform of the two functions g_1 and g_1^{tr} will depict peaks at classical actions and $\hbar$ corrections are obtained from the amplitude of these peaks. However, in the case of signal given by $c(t)=\Sigma a_n\exp(i\omega_n t)$, it is now well known that the harmonic inversion method is very well suited and is much more powerful than the conventional Fourier transform to extract unknown frequencies ω_n and amplitudes a_n [20]. In our case the signals are the two functions $g_1(\zeta)$ and $g_1^{\mathrm{tr}}(\zeta)$, which are of the form $\Sigma_l\mathcal{A}_l\mathcal{C}_l\sin(\zeta S_l+\phi_l)$ besides contributions from all other types of orbits (ghost, continuous family, etc.).

C. $\hbar$ corrections for $G(\mathbf{q},\mathbf{q}_0,2)$

Orbits having initial and final points at the nucleus (i.e., $\mathbf{q}=\mathbf{q}_0=\mathbf{0}$) are of special interest because they are involved in semiclassical estimation of the photoionization cross section [25,29], which can be directly compared to experimental results [30,31]. Even if the full $\hbar$ expansion of the cross section does not reduce to $G(\mathbf{0},\mathbf{0},2)$ contributions, all closed orbits are well known and classified, so that this case remains a nice example of $\hbar$ corrections for $G(\mathbf{q},\mathbf{q}_0,2)$.

The Fourier transforms of both functions $g_0(\zeta)$ (upper plot, solid line) and $g_1(\zeta)$ (lower plot, solid line), for scaled

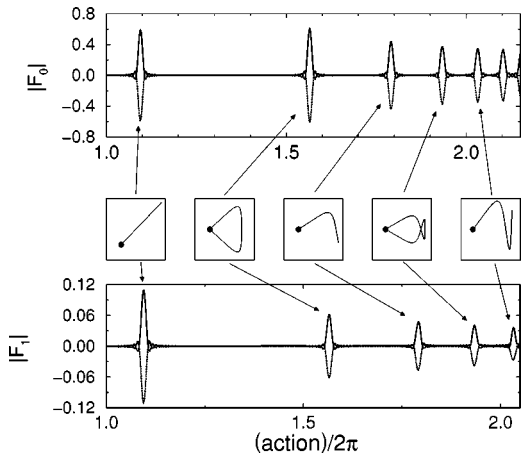

FIG. 3. Modulus of the windowed Fourier transforms F_0 (solid line, upper plot) and F_1 (solid line, lower plot), see Eq. (105), of the quantum functions g_0 (leading order in $\hbar$) and g_1 (first order $\hbar$ correction), see Eq. (104), associated with the quantum Green function $G(\mathbf{q},\mathbf{q}_0,2)$ in the case of the 2D hydrogen atom in a magnetic field and for $\mathbf{q}=\mathbf{q}_0=\mathbf{0}$ (see Sec. VI for all details). As expected from semiclassical formula (25), peaks are appearing at action (i.e., $\int \mathbf{p}\, d\mathbf{q}/2\pi$) corresponding to classical orbits having initial and final positions at the nucleus. For the first five ones, the trajectory in the (u,v) plane are also plotted, the nucleus being depicted by the black circle. The agreement with the semiclassical estimations of these functions (dotted lines) is excellent, even if discrepancies in the amplitude of last two peaks in the lower plot can be observed. These are actually a manifestation of limitation of the Fourier transform and not inaccurate calculations of the $\hbar$ corrections, as it is emphasized by the quantitative comparison (using harmonic inversion) displayed by Table II.

energy $\epsilon=-0.1$, are displayed in Fig. 3. More precisely, $g_0(\zeta)$, and $g_1(\zeta)$ being known only on a finite interval $[0,\zeta_{\max}]$, we have plotted the modulus of their windowed Fourier transforms, defined as follows:

$$F_0(s)=\frac{6}{(\zeta_{\max})^3}\int_0^{\zeta_{\max}} d\zeta\,\zeta(\zeta_{\max}-\zeta)g_0(\zeta)e^{-i2\pi s\zeta},$$

$$F_1(s)=\frac{6}{(\zeta_{\max})^3}\int_0^{\zeta_{\max}} d\zeta\,\zeta(\zeta_{\max}-\zeta)g_1(\zeta)e^{-i2\pi s\zeta}. \tag{105}$$

As expected, they depict peaks at the classical actions of closed orbits, whose trajectories in (u,v) plane have been inserted in the figure, the black circle corresponding to the nucleus position. In the figure, the dotted lines corresponds to the semiclassical estimations of the same functions using the classical properties given by Table I. The closed orbits being either half of a periodic orbit or a periodic orbit, we label a given close orbit with the four-disk code of the corresponding periodic orbit [32,33].

For the leading order in $\hbar$ (upper plot), as expected, the agreement between the quantum results and the semiclassical estimation is excellent. For the first order $\hbar$ correction, the agreement is very good, but one can notice that there is a discrepancy for the amplitude of the last two peaks. This is not due to errors or inaccurate calculations in the semiclassical estimation, but rather a manifestation of the limitations of the Fourier transform. To emphasize this point, we have used the harmonic inversion to extract, for each of these orbits, the $\hbar$ correction coefficients $\mathcal{C}_l^{HI}$, from the quantum function $g_1(\zeta)$. The results are compared to the classical calculation $\mathcal{C}_l$ in Table II. The agreement is excellent, the relative error on the amplitude being lower than 10^{-2}. As usual, the phase extracted using harmonic inversion, being the most sensitive quantity, the agreement on the sign of the $\mathcal{C}_l$, rather nice for the first four orbits, decreases rapidly. Finally, one must mention that this good agreement between quantum and semiclassical calculations has also been found when considering quantum Green's functions $G(\mathbf{q},\mathbf{q}_0,2)$ with other initial or final points.

D. $\hbar$ corrections for Tr $G(\mathbf{q},\mathbf{q},2)$

Still working at scaled energy $\epsilon=-0.1$, Fig. 4 depicts the modulus of the windowed Fourier transforms of $g_0^{\mathrm{tr}}(\zeta)$ and $g_1^{\mathrm{tr}}(\zeta)$, F_0^{tr} (upper plot, solid line), and F_1^{tr} (lower plot, solid line), defined, as previously, as follows:

$$F_0^{\mathrm{tr}}(s)=\frac{6}{(\zeta_{\max})^3}\int_0^{\zeta_{\max}} d\zeta\,\zeta(\zeta_{\max}-\zeta)g_0^{\mathrm{tr}}(\zeta)e^{-i2\pi s\zeta},$$

$$F_1^{\mathrm{tr}}(s)=\frac{6}{(\zeta_{\max})^3}\int_0^{\zeta_{\max}} d\zeta\,\zeta(\zeta_{\max}-\zeta)g_1^{\mathrm{tr}}(\zeta)e^{-i2\pi s\zeta}. \tag{106}$$

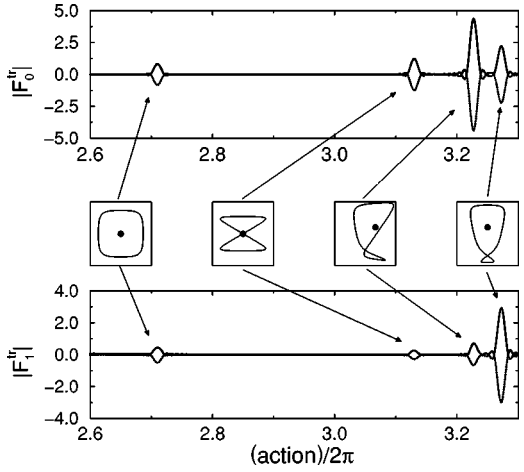

FIG. 4. Modulus of the windowed Fourier transforms F_0^{tr} (solid line, upper plot) and F_1^{tr} (solid line, lower plot), see Eq. (106), of the quantum functions g_0^{tr} (leading order in $\hbar$) and g_1^{tr} (first order $\hbar$ correction), see Eq. (104), associated with the trace of the quantum Green's function Tr $G(\mathbf{q},\mathbf{q},2)$ in the case of the 2D hydrogen atom in a magnetic field (see Sec. VI for all details). As expected from semiclassical formula (65), peaks are appearing at action (i.e., $\oint \mathbf{p}\, d\mathbf{q}/2\pi$) corresponding to classical periodic orbits, whose trajectories in the (u,v) plane are plotted (the nucleus being depicted by the black circle). The agreement with the semiclassical estimation (dotted lines) is excellent, as it is emphasized by the quantitative comparison (using harmonic inversion) displayed by Table IV.

TABLE I. Classical properties of closed orbits involved in the semiclassical expansion of the quantum Green's function $G(\mathbf{q},\mathbf{q}_0,2)$ of the 2D hydrogen atom in a magnetic field, for the case $\mathbf{q}=\mathbf{q}_0=\mathbf{0}$. Because each closed orbit corresponds either to a half-periodic orbit or a periodic orbit, we have labeled them with the four-disk code of the corresponding periodic orbit [32,33]. Their trajectories in the (u,v) plane are shown in Fig. 3. S_l is the reduced action (i.e., $\int \mathbf{p}\, d\mathbf{q}/2\pi$), T_l is the period, $\mathcal{A}_l$ is the leading semiclassical amplitude, $\tilde{\nu}_l$ is the Maslov index, $\mathcal{C}_l$ is the first order $\hbar$ correction, given by the sum $C_1(\mathbf{0},\mathbf{0},T_l)+C_1^{T\to E}(\mathbf{0},\mathbf{0},T_l)$, see Eq. (91).

Code	S_l	T_l	$\mathcal{A}_l$	$\tilde{\nu}_l$
$\overline{13}$	1.094 570 5	2.425 093 3	0.295 342 6	1
$\overline{1243}$	1.564 998 2	3.600 137 4	0.152 365 0	2
$\overline{121343}$	1.791 060 7	4.286 257 7	0.109 503 9	3
$\overline{12124343}$	1.933 522 1	4.796 775 8	0.093 368 7	4
$\overline{1212134343}$	2.031 948 2	5.214 323 3	0.086 142 0	5

Code	$C_1(\mathbf{0},\mathbf{0},T_l)$	$C_1^{T\to E}(\mathbf{0},\mathbf{0},T_l)$	$\mathcal{C}_l$
$\overline{13}$	−0.202 769 9	0.016 539 4	−0.186 230 5
$\overline{1243}$	−0.119 409 3	0.019 741 2	−0.099 668 1
$\overline{121343}$	−0.148 282 2	0.041 175 5	−0.107 106 7
$\overline{12124343}$	−0.172 990 6	0.071 748 0	−0.101 242 7
$\overline{1212134343}$	−0.192 904 3	0.117 464 5	−0.075 439 8

The trajectories in the (u,v) plane associated with the peaks are also plotted in the figure. The classical properties of the corresponding periodic orbits are displayed by Table III. Again the agreement is excellent between the quantum results (solid lines) and the semiclassical estimation (dotted lines). The quantitative comparison between the classical coefficients $\mathcal{C}_l^{\mathrm{tr}}$ and the values $\mathcal{C}_l^{HI}$ extracted from the quantum function $g^{\mathrm{tr}}(\zeta)$ is given in Table IV. The agreement is excellent for the amplitude of the coefficients and is rather good for their phases, which emphasized the validity of the semiclassical formula developed in the preceding sections, especially the additional term arising from the Jacobian describing the change from the Cartesian to local (along the periodic orbit) coordinates [see Eq. (48)] and which contributes to a large part of the $\hbar$ correction for the present orbits.

TABLE II. Numerical comparison between the theoretical $\hbar$ corrections $\mathcal{C}_l$ for the quantum Green's function $G(\mathbf{q},\mathbf{q}_0,2)$ of the 2D hydrogen atom in a magnetic field, for the case $\mathbf{q}=\mathbf{q}_0=\mathbf{0}$ and the numerical coefficients $\mathcal{C}_l^{HI}$ extracted from exact quantum function $g_1(\zeta)$ [Eq. (104)] using harmonic inversion (taking into account multiplicity). The agreement is excellent for the amplitudes and rather nice on the phases, thus emphasizing the validity of the present theory. That the agreement becomes less good for the last orbit only shows the limitations of the harmonic inversion method, which usually appear on the phase.

Code	$\mathcal{C}_l$	$\lvert\mathcal{C}_l^{HI}\rvert$	Rel. error	$\arg \mathcal{C}_l^{HI}$
$\overline{13}$	−0.186 230 5	0.1864	$\approx 8\times10^{-4}$	$1.002\times\pi$
$\overline{1243}$	−0.099 668 1	0.0995	$\approx 2\times10^{-3}$	$1.01\times\pi$
$\overline{121343}$	−0.107 106 7	0.1072	$\approx 9\times10^{-4}$	$1.02\times\pi$
$\overline{12124343}$	−0.101 242 7	0.1016	$\approx 4\times10^{-3}$	$1.04\times\pi$
$\overline{1212134343}$	−0.075 439 8	0.0761	$\approx 9\times10^{-3}$	$1.14\times\pi$

TABLE III. Classical properties of periodic orbits involved in the semiclassical expansion of the trace of the quantum Green's function $\mathrm{Tr}\, G(\mathbf{q},\mathbf{q},2)$ of the 2D hydrogen atom in a magnetic field. Their trajectories in the (u,v) plane are shown in Fig. 4. S_l^{tr} is the reduced action (i.e., $\oint \mathbf{p}\, d\mathbf{q}/2\pi$), T_l is the period, $\mathcal{A}_l^{\mathrm{tr}}$ is the leading semiclassical amplitude, μ_l is the Maslov index, $\mathcal{C}_l^{\mathrm{tr}}$ is the first order $\hbar$ correction, given by the sum $C_1(T_l)+C_1^{T\to E}(T_l)$, see Eq. (98).

Code	S_l^{tr}	T_l^{tr}	$\mathcal{A}_l^{\mathrm{tr}}$	μ_l
$\overline{1234}$	2.709 851 3	6.204 155 6	0.827 881 4	4
$\overline{1243}$	3.129 996 4	7.200 274 7	0.616 496 8	4
$\overline{12434}$	3.227 168 1	7.541 640 6	0.548 479 1	5
$\overline{123434}$	3.272 238 1	7.748 406 8	0.555 880 6	6

Code	$C_1(T_l)$	$C_1^{T\to E}(T_l)$	$\mathcal{C}_l^{\mathrm{tr}}$
$\overline{1234}$	−0.622 577	0.026 912	−0.595 665
$\overline{1243}$	0.166 821	0.051 665	0.218 486
$\overline{12434}$	−0.203 536	0.058 541	−0.144 995
$\overline{123434}$	−1.417 05	0.072 41	−1.344 64

VII. CONCLUSION

In summary, we have explained in this paper how to effectively compute $\hbar$ corrections in the semiclassical expansions of the propagator $K(\mathbf{q},\mathbf{q}_0,T)$, its trace $K(T)$, the quantum Green's function $G(\mathbf{q},\mathbf{q}_0,E)$ and its trace $G(E)$ for chaotic systems with smooth potential. The method is based on the classical Green's functions associated to the relevant trajectories, that is either going from $\mathbf{q}$ to $\mathbf{q}_0$ in the propagator case or periodic orbits for $K(T)$, together with adapted boundary conditions. We have shown how all quantities can be obtained by integrating, using the standard Runge-Kutta method, sets of differential equations. We have also shown

TABLE IV. Numerical comparison between the theoretical $\hbar$ corrections $\mathcal{C}_l^{\mathrm{tr}}$ for the trace of the quantum Green's function $\mathrm{Tr}\, G(\mathbf{q},\mathbf{q},2)$ of the 2D hydrogen atom in a magnetic field and the numerical coefficients $\mathcal{C}_l^{HI}$ extracted from exact quantum function $g_1^{\mathrm{tr}}(\zeta)$ [Eq. (104)] using harmonic inversion (taking into account multiplicity). The agreement is excellent for the amplitudes and rather nice on the phases, thus emphasizing the validity of the present theory, especially the additional term due to the transformation from the Cartesian coordinates to the local frame along the periodic orbit [see Eq. (48)].

Code	$\mathcal{C}_l^{\mathrm{tr}}$	$\lvert\mathcal{C}_l^{HI}\rvert$	Rel. Error	$\arg \mathcal{C}_l^{HI}$
$\overline{1234}$	−0.595 665	0.5958	$\approx 2\times10^{-4}$	$1.005\times\pi$
$\overline{1243}$	0.218 486	0.2178	$\approx 3\times10^{-3}$	$0.04\times\pi$
$\overline{12434}$	−0.144 995	0.147	$\approx 1\times10^{-2}$	$0.93\times\pi$
$\overline{123434}$	−1.344 64	1.347	$\approx 2\times10^{-3}$	$0.98\times\pi$

that in the derivation of the semiclassical expansion for $K(T)$ [and thus $G(E)$], starting from the Feynman path integral, one must take into account additional terms, which affect only $\hbar$ correction coefficients. This is emphasized by the excellent agreement observed when comparing, in the case of the 2D hydrogen atom in a magnetic field, our theoretical results with the numerical coefficients extracted from exact quantum data, using the harmonic inversion. Obviously, there are still many points to be developed. Besides the few cases, such as self-retracing orbits or continuous families of orbits, needing specific extensions, it would be very interesting to understand how to include continuous and discrete symmetries. Also, going into the extended phase space $(\mathbf{q},t,\mathbf{p},-E)$ [22], it would be possible to get a better understanding of similarities observed between the differential sets leading, on one side to the $\hbar$ corrections for the propagator and its trace and, on the other side to the additional terms arising in the $\hbar$ corrections for the quantum Green's function and its trace.

ACKNOWLEDGMENTS

The author thanks D. Delande for fruitful discussions and for his kind support during this work, especially for numerous suggestions which led to the present form. The author also thanks M. Kuś for useful discussions. Laboratoire Kastler Brossel is laboratoire de l'Université Pierre et Marie Curie et de l'Ecole Normale Supérieure, Unité Mixte de Recherche 8552 du CNRS.

APPENDIX: FEW PROPERTIES OF $M(T)$

In this Appendix, we consider an isolated unstable periodic orbit of period T. We shall use the notations $\mathbf{e}_\parallel$ and $\mathbf{e}_\perp$ for the units vectors, which are, respectively, parallel to the flow and perpendicular to the energy shell at the initial point. From Hamilton's equations, we have that $M(T)\cdot\mathbf{e}_\parallel=\mathbf{e}_\parallel$, i.e., $\mathbf{e}_\parallel$ is an eigenvector of the matrix $M(T)$ for the eigenvalue 1. The symplectic equation fulfilled by $M(T)$, namely, $M(T)^\top\cdot\Sigma\cdot M(T)=\Sigma$, implies that, if $\mathbf{e}_i$ and $\mathbf{e}_j$ are two eigenvectors for the eigenvalues λ_i and λ_j, we have the following properties:

$$M(T)^\top\cdot(\Sigma\mathbf{e}_i)=\frac{1}{\lambda_i}(\Sigma\mathbf{e}_i),$$
$$(\lambda_i\lambda_j-1)\mathbf{e}_i^\top\Sigma\mathbf{e}_j=0, \tag{A1}$$

showing thus that $1/\lambda_i$ is an eigenvalue of $M(T)^\top$ and, from that, of $M(T)$. In addition, $M(T)$ being a real matrix, $\overline{\lambda_j}$ and $1/\overline{\lambda_j}$ are also eigenvalues of $M(T)$, so that the nontrivial eigenvalues (i.e., $\neq 1$) either fall in the $(\lambda,1/\lambda)$ pair or in quadruplet $(\lambda,1/\lambda,\overline{\lambda},1/\overline{\lambda})$.

In the case of $\mathbf{e}_i=\mathbf{e}_\parallel$, the two preceding equations (A1) imply that $\mathbf{e}_\perp$ is an eigenvector of $M(T)^\top$ [but not necessarily of $M(T)$] for the eigenvalue 1 and that for every $\lambda_j\neq 1$, $\mathbf{e}_j$ is an orthogonal to $\mathbf{e}_\perp$. In the basis $(\mathbf{e}_\parallel,\mathbf{e}_\perp,\mathbf{e}_1,\ldots,\mathbf{e}_{2f-2})$, $M(T)$ entries then read

$$M(T)=\begin{bmatrix} 1 & \alpha_\parallel & 0 & 0 & \cdots & 0 \\ 0 & 1 & 0 & 0 & \cdots & 0 \\ 0 & \alpha_1 & \lambda_1 & 0 & \cdots & 0 \\ 0 & \alpha_2 & 0 & \lambda_2 & \cdots & 0 \\ \vdots & \vdots & \vdots & \vdots & \ddots & \vdots \\ 0 & \alpha_{2f-2} & 0 & 0 & \cdots & \lambda_{2f-2} \end{bmatrix}, \tag{A2}$$

where we have supposed that all eigenvalues are simple. For degenerated eigenvalues, $M(T)$ would be block diagonal. For a generic periodic orbit, $\alpha_\parallel$ and α_i are nonvanishing emphasizing thus that $\mathbf{e}_\perp$ is not an eigenvector of $M(T)$. Introducing the vector $\tilde{\mathbf{e}}_\perp$ defined as follows:

$$\tilde{\mathbf{e}}_\perp=\mathbf{e}_\perp+\sum_{j=1}^{2f-2}\beta_j\mathbf{e}_j \quad \text{with} \quad \beta_j=\frac{\alpha_j}{1-\lambda_j} \tag{A3}$$

one immediately gets that

$$M(T)\tilde{\mathbf{e}}_\perp=\tilde{\mathbf{e}}_\perp+\alpha_\parallel\mathbf{e}_\parallel. \tag{A4}$$

In the case $\alpha_\parallel=0$, we have thus found another eigenvector for the eigenvalue 1, which means that a small displacement of initial conditions in the $\tilde{\mathbf{e}}_\perp$ direction leads to another periodic motion with the same period T, and thus that the periodic orbit is actually embedded in a continuous family. Indeed, using notations from Sec. V, one can show that

$$\mathbf{X}^{(1)}(0)=-\frac{\|\dot{\mathbf{X}}\|}{\alpha_\parallel}\tilde{\mathbf{e}}_\perp \tag{A5}$$

so that we have

$$\alpha_\parallel=\|\dot{\mathbf{X}}\|^2\partial_E T. \tag{A6}$$

In Sec. V, one needs to compute derivatives with respect to the period T of $\det[m(T)-\mathbb{1}]$, whose expression in terms of the nontrivial eigenvalues of the monodromy matrix reads

$$\det[m(T)-\mathbb{1}]=\prod_{j=1}^{2f-2}(\lambda_j-1). \tag{A7}$$

Introducing $\mathcal{P}_\parallel$ and $\mathcal{P}_\perp$ the projectors on the directions $\mathbf{e}_\parallel$ and $\mathbf{e}_\perp$, more precisely,

$$\mathcal{P}_\parallel=\mathbf{e}_\parallel\cdot\mathbf{e}_\parallel^\top \quad \text{and} \quad \mathcal{P}_\perp=\mathbf{e}_\perp\cdot\mathbf{e}_\perp^\top \tag{A8}$$

ones defines the matrix $N(T)$ as follows:

$$N(T)=M(T)-(\mathbb{1}-\mathcal{P}_\parallel-\mathcal{P}_\perp). \tag{A9}$$

In the basis $(\mathbf{e}_\parallel,\mathbf{e}_\perp,\mathbf{e}_1,\ldots,\mathbf{e}_{2f-2})$, using orthogonality between $\mathbf{e}_\perp$ and $\mathbf{e}_j$, entries of $N(T)$ read

$$N(T)=\begin{bmatrix} 1 & \alpha_{\parallel} & \gamma_1 & \gamma_2 & \cdots & \gamma_{2f-2} \\ 0 & 1 & 0 & 0 & \cdots & 0 \\ 0 & \alpha_1 & \lambda_1-1 & 0 & \cdots & 0 \\ 0 & \alpha_2 & 0 & \lambda_2-1 & \cdots & 0 \\ \vdots & \vdots & \vdots & \vdots & \ddots & \vdots \\ 0 & \alpha_{2f-2} & 0 & 0 & \cdots & \lambda_{2f-2}-1 \end{bmatrix}, \tag{A10}$$

where $\gamma_j=\mathbf{e}_{\parallel}^{\top}\cdot\mathbf{e}_j$, which actually could be related to the α_j, but this is not necessary in our case. This shows that the determinant of $N(T)$ is exactly $\Pi_{j=1}^{2f-2}(\lambda_j-1)$. The main advantage of the matrix $N(T)$ is that its expression (A9) does not involve the eigenvectors or the eigenvalues of $M(T)$, so that its determinant can be directly computed, without the diagonalization stage required when getting $\det[m(T)-\mathbb{1}]$ through the eigenvalues λ_j. Furthermore, derivatives of $\ln\det N(T)$ with respect to the period T are also straightforward to obtain, knowing derivatives of $M(T)$ and of $\dot{\mathbf{X}}(T)$, whereas derivatives of λ_j would require the knowledge of those of the eigenvectors $\mathbf{e}_j$.

[1] M. C. Gutzwiller, *Chaos in Classical and Quantum Mechanics* (Springer-Verlag, New York, 1990).
[2] J. H. Van Vleck, Proc. Natl. Acad. Sci. U.S.A. **14**, 178 (1928).
[3] M. Brack and R. K. Bhaduri, *Semiclassical Physics* (Addison-Wesley, Reading, MA, 1997).
[4] H. Friedrich and D. Wintgen, Phys. Rep. **183**, 37 (1989).
[5] D. Delande, in *Chaos and Quantum Physics*, edited by M.-J. Giannoni, A. Voros and J. Zinn-Justin, Les Houches Summer School, Session LII (North-Holland, Amsterdam, 1991).
[6] G. S. Ezra, K. Richter, G. Tanner, and D. Wintgen, J. Phys. B **24**, L413 (1991).
[7] P. Gaspard and S. A. Rice, Phys. Rev. A **48**, 54 (1993).
[8] B. Grémaud and P. Gaspard, J. Phys. B **31**, 1671 (1998).
[9] D. S. Saraga and T. S. Monteiro, Phys. Rev. Lett. **81**, 5796 (1998).
[10] L. A. Bunimovitch, Commun. Math. Phys. **65**, 295 (1979).
[11] P. Cvitanović and B. Eckhardt, Phys. Rev. Lett. **63**, 823 (1989).
[12] P. Gaspard and D. Alonso, Phys. Rev. A **47**, R3468 (1993).
[13] P. Gaspard, D. Alonso, and I. Burghardt, Adv. Chem. Phys. **90**, 105 (1995).
[14] E. B. Bogomolny, U. Gerland, and C. Schmidt, Phys. Rev. E **59**, R1315 (1999).
[15] S. C. Creagh and R. G. Littlejohn, Phys. Rev. A **44**, 836 (1991).
[16] S. C. Creagh and R. G. Littlejohn, J. Phys. A **25**, 1643 (1992).
[17] G. Vattay and P. E. Rosenqvist, Phys. Rev. Lett. **76**, 335 (1996).
[18] B. Eckhardt and D. Wintgen, J. Phys. A **24**, 4335 (1991).
[19] J. Main, K. Weibert, and G. Wunner, Phys. Rev. E **58**, 4436 (1998).
[20] J. Main, Phys. Rep. **316**, 233 (1999).
[21] K. Weibert, J. Main, and G. Wunner, Eur. Phys. J. D **12**, 381 (2000).
[22] R. G. Littlejohn, J. Math. Phys. **31**, 2952 (1990).
[23] R. Marcinek and D. Delande, Phys. Rev. A **62**, 062704 (2000).
[24] T. Jonckheere, B. Grémaud, and D. Delande, Phys. Rev. Lett. **81**, 2442 (1998).
[25] E. P. Bogomolny, Zh. Éksp. Teor. Fiz. **96**, 487 (1989) [Sov. Phys. JETP **69**, 275 (1989)].
[26] M. J. Englefield, *Group Theory and the Coulomb Problem* (Wiley, New York, 1972).
[27] C. C. Martens, R. L. Waterland, and W. P. Reinhardt, J. Chem. Phys. **90**, 2328 (1989).
[28] J. M. Robbins, Phys. Rev. A **40**, 2128 (1989).
[29] J. Gao and J. B. Delos, Phys. Rev. A **46**, 1455 (1992).
[30] A. Holle, J. Main, G. Wiebusch, H. Rottke, and K. H. Welge, Phys. Rev. Lett. **61**, 161 (1988).
[31] J. Main, G. Wiebusch, K. Welge, J. Shaw, and J. B. Delos, Phys. Rev. A **49**, 847 (1994).
[32] B. Eckhardt and D. Wintgen, J. Phys. B **23**, 355 (1990).
[33] K. T. Hansen, Phys. Rev. E **51**, 1838 (1995).